Harnessing the power of fluorescence to characterize biomolecular condensates

Benjamin Levin[a,†], Matthäus Mittasch[b,†], Beatriz Ferreira Gomes[b], John Manteiga[a], Avinash Patel[b], Alicia Zamudio[a,‡], Oliver Beutel[b], and Diana M. Mitrea[a,*]

[a]*Dewpoint Therapeutics, Boston, MA, United States*

[b]*Dewpoint Therapeutics GMBH, Dresden, Germany*

**Corresponding author: e-mail address: dmitrea@dewpointx.com*

1 Introduction

Spatial and temporal organization of cellular processes is achieved via selective compartmentalization of macromolecules (i.e., proteins, DNA, RNA) and metabolites within stable, membrane-bounded organelles, or within metastable membrane-less organelles. While both types of organelles have similar intracellular localizations (freely diffusing or tethered to membranes, chromatin, or the cytoskeleton) their key differences are highlighted in Fig. 1. Membrane-less organelles, also referred to as biomolecular condensates, form through the process of phase separation, where one or more types of macromolecules condense into a dense phase, and become depleted from the surrounding milieu. The local concentration inside the condensate is often orders of magnitude higher with respect to the outside (reviewed in Hyman, Weber, & Julicher, 2014); this sharp change in concentration represents the phase boundary of the condensate (Fig. 1). They assemble and disassemble dynamically in response to environmental changes, resulting in changes to signalling and biochemical reaction outputs (reviewed in Banani et al., 2016; Mitrea & Kriwacki, 2016; Sabari, Dall'Agnese, & Young, 2020). Formation of biomolecular condensates

[†]These authors contributed equally.

[‡]Current address: Department of Neuroscience, Genentech, 1 DNA Way, South San Francisco, CA 94080, United States.

Methods in Microbiology, ISSN 0580-9517, https://doi.org/10.1016/bs.mim.2020.11.005

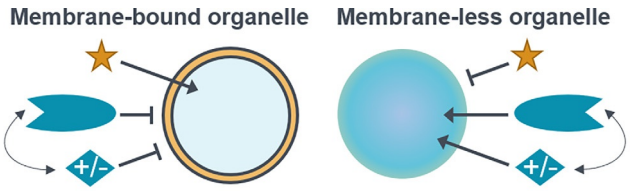

What is the boundary?	Lipid bilayer	Phase boundary
What determines permeability?	Hydrophobicity	Miscibility and/or interaction with the condensate components
How does it respond to environmental queues?	Through lipid regulatory mechanisms	Through direct interaction
How does it form?	Membrane biogenesis	Phase separation

FIG. 1

Differences between a membrane-bound and a membrane-less organelle. (Top) Schematic demonstrating the first two rows of the table (bottom). (Left) A membrane-bound organelle is bound by a lipid bilayer (double outline). Due to the hydrophobicity of the membrane, it is permeable to most small hydrophobic molecules (star) but not permeable to most proteins (oval) or small charged molecules (diamond). (Right) A membrane-less organelle differentiates from its surroundings due to a sharp change in concentration/density of its components at the phase boundary. Molecules that are miscible and/or interact with the condensate components (indicated by blue colouring) will partition into a condensate, while others (indicated by gold colouring) will not.

has been reported in all walks of life, from animals, plants and fungi to bacteria and viruses (reviewed in Alberti & Dormann, 2019; Cuevas-Velazquez & Dinneny, 2018).

Biomolecular condensates play a wide range of functional roles (see Table 1) including, but not limited to, regulation of transcription (Boija et al., 2018; Ladouceur et al., 2020; Li et al., 2020), ribosome biogenesis (Brangwynne et al., 2011; Feric et al., 2016; Mitrea, Cika, et al., 2018; Riback et al., 2020), stress response (Boothby et al., 2017; Riback et al., 2017), spatial segregation of transcripts (Brangwynne et al., 2009; Lee, Occhipinti, & Gladfelter, 2015; Wang et al., 2014), membrane biogenesis and trafficking (reviewed in Zhao & Zhang, 2020), regulation of protein degradation (Bouchard et al., 2018; Yasuda et al., 2020), and signal transduction (Li et al., 2012). Misregulation of biomolecular condensates has been associated with a number of diseases, such as neurodegeneration, cancer and infectious diseases (reviewed in Alberti & Dormann, 2019). Consequently, understanding how to predictably modulate the function of macromolecular condensates is critical for their exploitation as therapeutic targets.

Biomolecular condensation is driven by multivalent interactions, oftentimes weak in nature, between proteins (Li et al., 2012), nucleic acids (Jain & Vale, 2017) and combinations thereof (Mitrea et al., 2016; Molliex et al., 2015). Multivalency (reviewed in Mitrea et al., 2018) is encoded as repetitive short linear motifs

Table 1 Biomolecular condensates discussed in this chapter and their functions.

Condensate	Function	References
Nucleolus	Ribosome biogenesis	Brangwynne, Mitchison, and Hyman (2011), Feric et al. (2016), Mitrea et al. (2018)
Transcriptional condensates	Transcription	Boija et al. (2018), Cho et al. (2018), Chong et al. (2018)
Bacterial nucleoid	Transcription	Ladouceur et al. (2020), Stracy et al. (2015)
P-body	RNA metabolism	Hubstenberger et al. (2017), Xing, Muhlrad, Parker, and Rosen (2020)
Stress granule	Stress response	Jain et al. (2016), Patel et al. (2015), Riback et al. (2017)
Centrosome	Microtubule organization	Mittasch et al. (2020), Woodruff et al. (2017)
Nuclear speckles	Splicing	Fei et al. (2017)

within intrinsically disordered protein regions (Nott et al., 2015; Pak et al., 2016), repetitive structured protein domains (Li et al., 2012), nucleotide sequence bias in unstructured regions of nucleic acids (Boeynaems et al., 2019), and/or repetitive structural features in nucleic acids (Langdon et al., 2018).

The field of studying biomolecular condensates resides at the intersection between cell biology, microbiology, polymer and soft matter physics, biophysics and structural biology. Through this collective knowledge, an understanding has started for the underlying rules for assembly/disassembly of biomolecular condensates, as well as rules for correlating condensate material properties with biological function. For example, the sequence grammar, such as structural domains and amino acid bias in intrinsically disordered regions (IDR), determines the composition and ultimately the function of the condensate (Wang et al., 2018). Further, the fine balance between the strength and valency of interactions and the stoichiometric ratio of interacting species within the condensates dictate the composition, material properties and stability of condensates (Banani et al., 2016; Riback et al., 2020). Simply put, interactions on the microscale (Ångstrom to nanometre) affect material properties of the biomolecular condensates on the mesoscale (hundreds of nanometres to micrometres). Due to their wide applications, fluorescence-based methods (reviewed in Mitrea, Chandra, et al., 2018) are extensively used in the field to interrogate structural, dynamic, viscoelastic and functional features of biomolecular condensates (Fig. 2).

In this chapter, the recent fluorescence-based technological advances employed in the characterization of biomolecular condensates are discussed. The basic principles of each technique are described, their advantages and applications are compared, as well certain limitations are discussed. This information should serve as

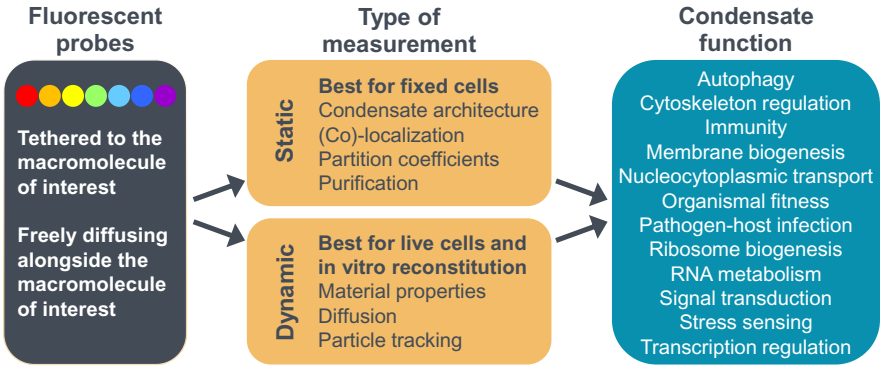

FIG. 2

Summary of applications of fluorescent probes to the study of biomolecular condensates.

a guide to select the appropriate technology for a given question under study. Finally, a discussion is provided on how these methods help to develop new classes of therapeutic agents that selectively target malfunctioning condensates.

2 Labelling methods

In order to fluorescently visualize a biomolecular condensate of interest, either in vitro, in living cultured cells or in vivo, one or more of its components are labelled, by direct tethering of a fluorophore to the molecule of interest (Fig. 2). This fluorophore allows for high signal-to-noise detection of the macromolecule(s) of interest, and quantitative analysis of parameters such as stoichiometry, dynamics, and spatiotemporal distribution.

Direct tethering methods are instrumental for the determination of the target molecule's spatial and temporal localization and provide information on the condensate's composition and the dynamic behaviour of the tagged molecule inside the condensate of interest. However, certain measurements, such as determination of bulk material properties of a condensate, can suffer from artefacts if the observed molecule interacts directly with the condensate milieu. Therefore, a second class of fluorescent probes is employed, which are not directly coupled to any condensate components.

Freely diffusing fluorescent probes which do not interact with the components of the condensate can be leveraged to interrogate the viscoelastic and physicochemical properties of the dense phase (Fig. 2). Such probes are often utilized as tracer molecules. They can be fluorescently tagged polymers (Wei et al., 2017), fluorescent beads (Elbaum-Garfinkle et al., 2015), genetically-encoded particles

(Delarue et al., 2018) or any other type of fluorescently labelled molecule that does not interact with any of the components of the condensate of interest (see Section 5).

2.1 Bioconjugation

The incorporation of fluorescent probes within biomolecules is a subgenre of bioconjugation chemistry. Fluorescent probes lay the foundation for visualizing, tracking, and quantifying molecular phenomena both in vivo and in vitro. The field co-evolved initially with description of antibody stained tissue sections (Coons, Creech, Jones, & Berliner, 1942) and flourished with the introduction of fluorescence activated cell sorting (FACS). The methodology developed to conjugate fluorescent small molecules applies directly to antibodies and other biomolecules. Bio-orthogonal approaches blossomed with the description, characterization, and utilization of the green fluorescent protein (GFP) from the jellyfish *Aequorea victoria* (Shimomura, Johnson, & Saiga, 1962). The impact of this contribution is emphasized by hundreds of fluorescent and chromogenic proteins found in the literature, and the 2008 Nobel Prize in Chemistry shared by Shimomura, Chalfie, and Tsien (https://www.nobelprize.org/prizes/chemistry/2008/summary).

Such methods for direct tethering of a fluorescent moiety to the biomolecule of interest, has enabled the study of biomolecular condensates composition and internal architecture, as well as material properties and dynamic behaviour of their components. This section will expand on genetic fusions, chemical labelling, and the labelling/detection of nucleic acids (summarized in Table 2).

Table 2 Fluorescent labelling techniques.

Protein labelling		Nucleic acid labelling	
Fluorescent proteins	Constitutively fluorescent proteins Photoconvertible proteins	In situ hybridization (ISH)	smFISH (with and without signal amplification)
Dye binding proteins	SNAP CLIP HALO TMP-tag	Genetically encoded	RNA binding proteins (MS2, U1A, etc.) RNA aptamers Molecular beacons rCAS9/dCAS13
Enzymatic labelling	Lipoic acid ligase Biotin ligase		
Unnatural amino acid labelling	Direct incorporation into the polypeptide chain		
Chemical labelling	Amine reactive derivatives Thiol reactive derivatives Carboxylic acids Aldehydes and ketones		

2.2 Genetically-encoded protein fluorescent tags

Genetic fusions come in two flavours: (1) proteins that are intrinsically fluorogenic (Fig. 3A), and (2) enzymes engineered to react irreversibly with substrates that are coupled to small fluorescent molecules, and consequently become fluorescent (Fig. 3B–E).

2.2.1 Constitutively fluorescent protein tags

One of the primary goals of genetic engineering for fluorescent proteins is to access new colours that expand the biological paint box accessible to the investigator. The topology of GFP and related proteins is well conserved. The primary structure is 11 β-strands surrounding an internal α-helix, and a chromophore which forms from amino acids 65–67 and matures in the presence of oxygen. Subtle changes to the sequence in and around the chromophore-forming amino acids modulate the excitation and emission spectrum of the fluorescent protein (Fig. 3A).

The palette of fluorescent proteins available to date broadly encompasses the visible and infrared spectrum, along with a selection of photoconvertible variants. Upon excitation with the appropriate wavelength, photoconvertible proteins undergo isomerization of the chromophore, which results in constitutive activation, colour conversion, and reversible "on/off" switching (Bourgeois & Adam, 2012). Colour-converting protein examples include Dendra2 (Gurskaya et al., 2006) and rsCherry (Stiel et al., 2008). Applications of these proteins extend to photolabelling of specific cellular regions, super resolution microscopy, FRET, single molecule tracking and nanoscopy (Bizzarri et al., 2010). Photoactivatable GFP was used to demonstrate protein mobility across the nuclear envelope and protein exchange within the lysosomal membrane (Patterson & Lippincott-Schwartz, 2002).

These genetically encoded fluorescent protein tags come in many variations in oligomeric state (i.e., monomeric, dimeric, tetrameric), chromophore maturation rates, pH stability, photoconversion capabilities, etc. Modulation of the environment surrounding the chromophore (hydrogen bonding network, π-stacking, etc.), not only influences the excitation and emission spectra, but also influences photostability, quantum yield, and brightness. These properties should be critically evaluated for compatibility with the desired application and scientific question asked. The community-editable database, fpbase.org (Lambert, 2019) catalogues the continuously expanding collection of fluorescent proteins and their properties; it serves as a great resource for selection of the appropriate genetically-encoded fluorescent protein for the desired application.

2.2.2 Bio-orthogonal labelling

Bio-orthogonal labelling refers to methods where a chemical reaction is initiated in living cells, and attaches a small molecule to a target protein. Several types of tags and chemical strategies have been developed to date, and researchers can select from them based on compatibility with their specific application. Here three categories of bio-orthogonal labelling will be discussed: (1) enzymes which are irreversibly

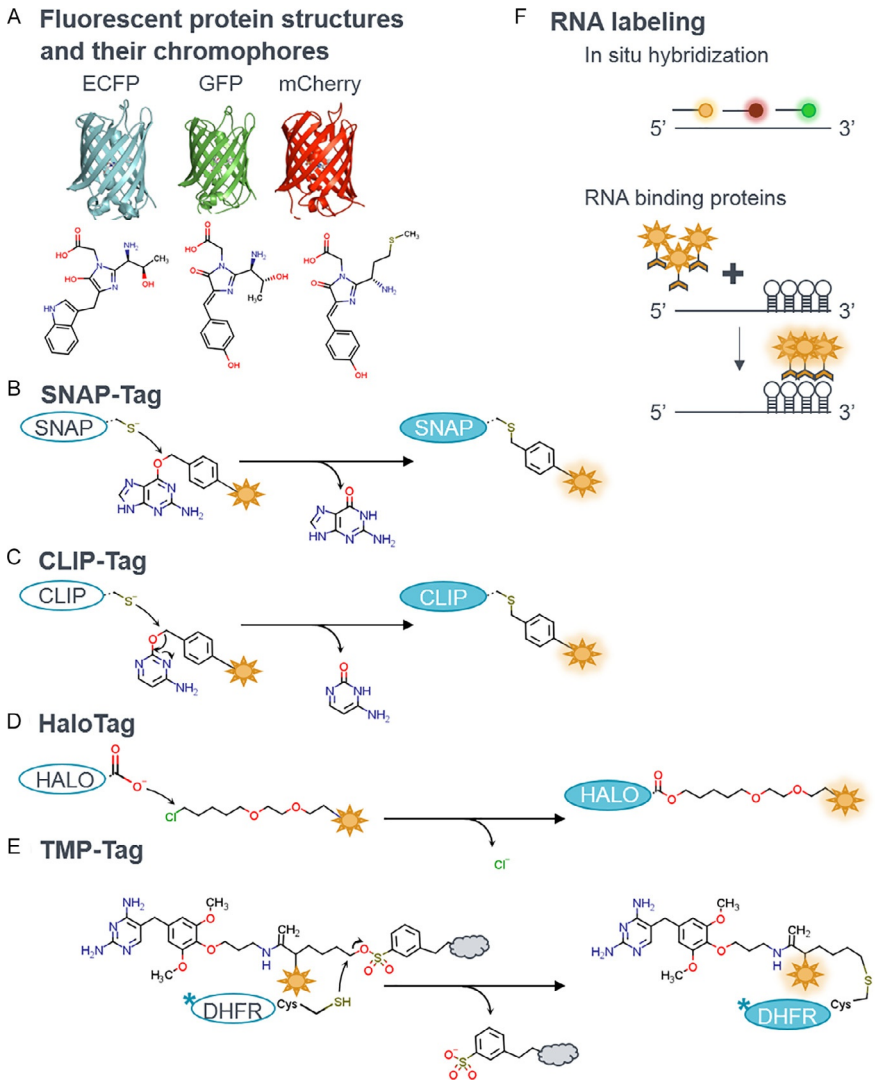

FIG. 3

Methods for fluorescent labelling of proteins and nucleic acids. (A) Structure of fluorescent proteins and their chromophores: enhanced cyan fluorescent protein (ECFP, PDB: 5OX8), GFP (PDB: 1EMA), and mCherry (PDB: 2H5Q). (B–E) Examples of genetic fusions and their mechanisms, where stars represent fluorophores, ovals represent the fusion proteins pre- (white) and post- (blue) conjugation represent quenchers. The asterisk (*) in E represents TMT engineered to accept ligands capable of being coupled covalently, but can interact with non-covalent ligands too. (F) Examples of RNA labelling (top) in situ hybridization of three differently tagged probes, and (bottom) RNA Binding Protein detection of RNA recognition sequence.

inhibited by binding to fluorescent conjugates (Fig. 3B–E), (2) enzyme-mediated labelling, and (3) unnatural amino acid incorporation.

2.2.2.1 Enzyme inhibition by fluorescent conjugates

Self-labelling tags are frequently used to combine the advantages of genetically-encoded tags with the flexibility of choosing fluorophores with different spectral and photophysical properties. The fluorophore is a small molecule inhibitor or binder to an enzyme fused in-frame to the protein of interest. They typically have fast kinetics to expand the applicability across in living cells and in vitro applications. Hallmarks of these fluorophore conjugates are that they have low unbound fluorescence; thereby, their contribution to background fluorescence is minimal. SNAP, CLIP and Halo tags (Fig. 3B–D) are used most frequently in the study of biomolecular condensates.

The SNAP- (Heinis, Schmitt, Kindermann, Godin, & Johnsson, 2006) and CLIP-tags (Fig. 3B–C) are engineered O^6-alkylguanine transferase (AGT) to eliminate native DNA binding to improve stability and reactivity (Gautier et al., 2008). SNAP (Fig. 3B) reacts with benzylguanine-tethered fluorophores, while CLIP (Fig. 3C) reacts with benzylcytosine derivatives. While these enzymes are similar, the high substrate specificity prevents cross-reactivity and allows them to be used simultaneously in both live-cell and in vitro systems. These tags are suitable for multiple applications, including static and dynamic measurements.

The HaloTag system (Fig. 3D) is engineered from the bacterial haloalkane dehalogenase enzyme from *Rhodococcus rhodochrous* (Los & Wood, 2007; Newman et al., 1999). The enzyme reacts with chloroalkane ligands, displacing the constitutively bound chloride. Under native conditions, His272 would act as a general base resulting in the release; however, mutation to Phe disrupts the regular catalytic activity. Similar to SNAP and CLIP, Halo has wide-ranging utility across in vitro and in vivo studies, including static and dynamic measurements.

The *E. coli* dihydrofolate reductase (ecDHFR) is selective for folate analogs like trimethoprim (TMP) (Miller, Cai, Sheetz, & Cornish, 2005), leading to the TMP-tag system (Fig. 3E). Early versions of the TMP fluorophore conjugates were not covalent but were suitable for tagging in living cells and in vitro. The second-generation TMP conjugates had significantly improved kinetics and photophysical properties (Calloway et al., 2007). Cornish and colleagues developed a mutant, ecDHFR L28C, capable of covalent modification in the presence of acrylamide-TMP-conjugate (Gallagher, Sable, Sheetz, & Cornish, 2009). These have been applied to molecular tracking in live cells and pulse-chase studies (Gallagher et al., 2009).

Genetically-encoded tags provide a wide range of advantages, from the wide selection of spectral and photophysical properties, to the compatibility with live-cell imaging and real-time tracking of molecular dynamics. However, they obligatorily add a sizable appendix to the protein of interest, which can affect the behaviour and function of the target of interest. For example, the tag can influence the molecular dynamics, sterically block interaction sites or lead to conformational changes. These interferences can result in altered temporal and spatial localization of the fusion

protein in the living cell, or change its interaction network. Therefore, the effects of the genetically-encoded tags should be thoroughly controlled for in the initial stages of experimental design.

Because phase separation is driven by multivalent interactions, adding additional valency is a particularly dangerous artefact that can be introduced by a genetically-fused tag. This occurs when the tag has the propensity to oligomerize. For example, GFP exhibits weak dimerization, which is often negligible when working with genetically-fused proteins in solution. However, in the context of a condensate, where local concentrations of the labelled protein can reach up to the millimolar range, GFP's additional dimerization interface can significantly influence phase behaviour. Such effects range from lowering the critical concentration for phase separation to changing the material properties, or even altering the photophysical properties of the fluorescent tag. These effects can be minimized by further weakening GFP–GFP interactions through site-directed mutagenesis of residues located at the dimerization interface (Feric et al., 2016).

2.2.2.2 Enzyme-mediated labelling

If the size of the fusion protein is the concern, it is possible to engineer a small acceptor peptide fusion that can be enzymatically delivered to a functionalized handle or conjugated fluorescent probe. For example, *E. coli* Biotin ligase (BirA) links biotin on an acceptor peptide's lysine. The standard sequence, GLNDIFEAQKIEWHE, is a minimal motif recognized by the enzyme. Avidin-fluorophore conjugates can then be used to label the modified acceptor. Ting and colleagues explored using biotin ligases from other organisms and found that they could expand the analogs tolerated for transfer, including those containing azide and alkyne functional groups (Slavoff, Chen, Choi, & Ting, 2008). Similarly, the Ting group engineered lipoic acid ligase (LipA) to recognize a 22 amino acid sequence. LipA catalyses a lysine residue's acylation on the acceptor peptide with azide or alkyne modified lipoic acid (Fernandez-Suarez et al., 2007). In contrast to the enzyme inhibitory labelling scheme (Fig. 3B–E), the ligases suffer from slower kinetics and turnover; in turn, they provide the advantage of a small size (less than two kilodaltons) which brings it in closer proximity and minimizes steric interference with the target. They can be used for both in vitro and live cell applications.

The least disruptive setup would be one where the dye is directly incorporated into the protein of interest, without adding a large appendage. Two such methods will be discussed below: unnatural amino acid incorporation, and post-synthesis chemical ligation.

2.2.2.3 Unnatural amino acids

Genetic code expansion enables the incorporation of non-canonical or unnatural amino acids (uAA) into growing, nascent polypeptides. In endogenous systems, the cell will incorporate the 20 natural amino acid residues using 61 codons, leaving the 3 remaining codons to terminate translation. Most organisms do not heavily utilize the amber stop codon, UAG, which has made it a prime target for identifying

orthogonal tRNA/aminoacyl-tRNA synthetase (aaRS) pairs that recognize the amber codon and tolerate desired amino acid composition (Nodling, Spear, Williams, Luk, & Tsai, 2019; Trotta, 2016). Direct encoding of uAAs offers specificity and freedom to place the fluorophore or reactive handle within a target protein with limited structural perturbations. This approach has several hurdles; aaRS/tRNA pairs must be identified or engineered for the host system. Incorporation rates can be low. The synthesis expense of the amino acids can be a barrier to their use in more extensive experiments. Continued expansion of the code is needed to incorporate more than one uAA. Chilkoti and colleagues demonstrated the utility of uAA incorporation to elastin-like polypeptides capable of photo-crosslinking. Droplet size was tunable across the nano- to mesoscale (Costa et al., 2018).

A major disadvantage of any genetically-encoded fluorescent protein is the need to introduce the modified target protein into the system. Time-efficient methods such as transient transfection lead to overexpression of the target protein, which, especially in the case of phase-separation proteins can lead to formation of ectopic, premature or artificial condensates (Nott et al., 2015). Methods that preserve the expression levels close to or at the endogenous levels, such as bacterial artificial chromosomes transgeneomics (Poser et al., 2008) or genome editing using CRISPR/Cas9 (Rodriguez-Rodriguez, Ramirez-Solis, Garza-Elizondo, Garza-Rodriguez, & Barrera-Saldana, 2019) are preferred, but require longer lag times.

For in vitro applications, the most straight-forward approach is to perform a post-synthesis chemical ligation of the desired fluorophore to a specific site on the polypeptide chain, as discussed below.

2.3 Chemical labelling with small molecule fluorophores

Post-production methods of incorporating fluorophores are largely driven by the target's amino acid composition. The most common chemistries are nucleophilic substitution reactions; acylations, and alkylations of primary amines (i.e., lysines and amino-terminus) and thiol side-chains. Acylation reactions are amine-reactive and form amides, thiourea, or sulphonamides. The most common alkylating agents are maleimides, predominantly reactive with sulfhydryl groups, and form thioether bonds. Cysteines are the primary target. However, the sulfhydryl groups can be added through thiolating reagents. When performing conjugation chemistry, there are practical considerations, such as the choice of reaction pH, buffer composition, and the desired location for the chemical conjugation (i.e., amino acid side chain, amino or carboxyl terminus). The conditions are more dependent on the chemistry employed, less on the choice of fluorophore, and limited by the target protein's stability. The reactivity can be biased for off-target residues using pH and the known pK_a of the side chain/terminus.

In vitro, the reduction of components enables the use of a unique dye per component. When designing experiments, the balance between labelling efficiency and random incorporation of the label is critical. Near stoichiometric labelling can often be achieved by conducting the reaction in slight excess of the label to target a single

available modification site. When more than one residue is likely to be modified, empirical trials are needed to ensure proper labelling efficiency and enable quantitative measurements. Transitions into the dense phase concentrate the target protein by orders of magnitude, and along with it the fluorescent probe, which can lead to photophysical changes of the fluorophore (Mitrea, Cika, et al., 2018). Additionally, a highly concentrated label can obscure the dynamics of a system. Sparce labelling of the target protein, for both in vitro and in vivo applications, reduces such artefacts (Liu et al., 2018; Mitrea, Cika, et al., 2018).

Chemical labelling is practical when studying in vitro systems. While it does not preclude the use in vivo, there are few examples of chemical labelling of intracellular proteins or RNA in live cells. In addition to the genetically-encoded tagging, described above, one of the most widely used techniques for fluorescently tagging proteins in cells is immunofluorescence.

2.4 Immunofluorescence

Immunofluorescence (IF) leverages the high affinity, high specificity interaction between a target protein and an antibody raised against the full length or portions of the target. Typically, the target protein is recognized by a specific primary antibody which is either directly conjugated to a fluorescent dye or further bound by a dye-conjugated secondary antibody. The first strategy offers the advantage of a lower background of non-specific binding, and the disadvantage of lower signal-to-noise and higher price tag. The second, less expensive strategy, offers enhanced signal-to-noise, provided by the signal amplification step from binding of the secondary antibody. A major advantage of IF-based methods is they allow for monitoring of endogenous proteins in cell culture and tissue samples without the need for overexpression or time-consuming genetic engineering. IF, however, is incompatible with live cell imaging, as the sample preparation requires fixation and permeabilization prior to labelling. Moreover, a cautionary note should be mentioned with respect to the fixation and permeabilization methods used, which, under certain circumstances, could result in disruption or other alterations of biomolecular condensates.

The fluorescence tethering methods described above are instrumental at visualizing proteins. In addition to proteins, however, nucleic acids are an abundant component of biomolecular condensates. Therefore, there is a need for visualizing their localization and track dynamics, similar to proteins. Methods for visualization of nucleic acids in living and fixed cells, as well as in vitro will be discussed in the next section.

2.5 Nucleic acid labelling

The growing toolbox for cellular painting is not complete without mentioning fluorophores for nucleic acids. Intercalating and non-intercalating dyes are readily available and easy to use, yet do not provide quantitative information and specificity for the type of DNA/RNA labelled. Often overlooked (or under-appreciated),

the bisbenzimide dyes, which are nearly ubiquitous in the literature, were developed by Hoechst AG in the early 1970s, and numbered as they were developed (Bucevicius, Lukinavicius, & Gerasimaite, 2018). These dyes are all excited by UV light and upon binding to DNA, their fluorescence increases approximately 30-fold (Adhikary, Buschmann, Muller, & Sauer, 2003; Han, Taulier, & Chalikian, 2005).

In situ hybridization methods rose out of Pardue and Gall's report in 1969 (Pardue & Gall, 1969) (Fig. 3F top). The current generations of single molecule fluorescent in situ hybridization (smFISH) rose from the Singer lab in 1998 (Femino, Fay, Fogarty, & Singer, 1998). In this technique, fluorescently labelled oligonucleotides are hybridized to their target DNA or RNA (Fig. 3F, top), and detected via fluorescence microscopy. Signal to noise challenges are overcome by using multiple oligos per RNA target, and/or coupling with a variety of signal amplification strategies. A few examples include FISH-STICs (Sinnamon & Czaplinski, 2014), MERFISH (Xia, Fan, Emanuel, Hao, & Zhuang, 2019), SABER-FISH (Kishi et al., 2019), etc. The most appropriate flavour of FISH for a particular application will have to take into account factors such as the need for: multiplexing, quantitative analysis, fixed versus live measurements, signal to noise, cost, availability of specialty fluorophores, compatibility with other types of sample preparation (i.e., IF), etc. For example, smFISH is superior for being highly quantitative, signal-to-noise issues can be overcome by coupling the hybridization probes with bright and stable fluorophores, and is compatible with IF techniques (Fusco et al., 2003). It is, however, not compatible with multiplexing applications. For such applications, MERFISH coupled with a branched DNA-amplification approach (Xia, Babcock, Moffitt, & Zhuang, 2019) or SABER-FISH, which uses signal amplification by exchange reaction (Kishi et al., 2019), are more advantageous. Special consideration should be given in the initial stage of the FISH probes design, to include factors such as melting temperature and free energy, as well as base composition and secondary structure of the oligo, which all contribute to the efficiency of hybridization and stability of the probe.

In living cells, techniques such as molecular beacons, aptamers, and stem-loop labelling are common strategies for visualizing RNAs. Single RNA loci were first visualized by Robinette in 1996 using a LacO array, and LacI protein fused to GFP (Robinett et al., 1996). RNA binding proteins fused to a fluorescent protein can bind to arrays of engineered stem-loops (Fig. 3F, bottom). This system can be multiplexed for specific recognition sites, and even tolerates split fluorescent proteins (Wu, Chen, & Singer, 2014). PP7 bacteriophage coat protein, MS2 coat protein, and U1A are a few members of this protein family, which recognize specific RNA structural features (Bertrand et al., 1998; Fusco et al., 2003; Wu et al., 2014). MS2 was used by Cisse and colleagues to probe the co-localization of the mediator complex and RNA polymerase II (Poll II) at sites of active transcription at a functional gene locus for *Esrrb*. They found that Mediator and Poll II form stable clusters indicative of biomolecular condensates. The mediator clusters and gene loci did not overlap but moved in concert with the transcriptional machinery (Cho et al., 2018).

Protein and nucleic acid labelling provide a platform to detect, track and purify these species and their binding partners. These applications will be discussed in the following section.

3 Condensate composition

The function and biophysical properties of biomolecular condensates are determined by their composition. The composition of a biomolecular condensate undergoes changes in response to alterations in the cellular microenvironment. For example, the proteome of the nucleolus (Andersen et al., 2005) and the stress granules (Aulas et al., 2017) are dynamically tuned with measurable differences between different types of transcriptional inhibition and stress, respectively. Understanding the rules for molecular networking within biomolecular condensates as a function of perturbation is paramount for their exploitation as therapeutic targets.

The biomolecular condensate network is composed of two types of macromolecules: scaffolds and clients. Scaffolds are multivalent components required for initiating phase separation, which create a macromolecular network that recruits and concentrates clients–molecules with lower valency that have an affinity for the condensate network (Banani et al., 2016) (Fig. 4). The ratio between the concentration of the macromolecule inside (dense phase) and outside (light phase) the biomolecular condensate is termed partition coefficient (Fig. 4A). Scaffold molecules are typically characterized by a higher valency and partition coefficient and lower dynamics (see Section 5)—imposed by their higher degree of connectivity within the network, when compared to client molecules (Xing et al., 2020). For example, the centrosome is a biomolecular condensate composed of a pair of centrioles surrounded by an amorphous matrix of proteins called pericentriolar material (PCM). Spindle-defective protein 5 (SPD-5) is the primary scaffold protein of the pericentriolar material, and is vital for centrosome maturation and mitotic spindle assembly in the zygote of *C. elegans*. In vitro, SPD-5 self-assembles to form condensates, via interactions between its coiled-coil domains (unpublished data). These condensates can specifically recruit PCM components (i.e., SPD-2, PLK-1, TPXL-1, ZYG-9, and tubulin) as clients, leading to in vitro microtubule nucleation (Woodruff et al., 2017).

Fluorescence-based methods, such as IF, fluorescent genetic tagging and FISH (described above) are used to visualize the partitioning of proteins and nucleic acids in biomolecular condensates, as a means to identify new components or validate components identified via omics methods, such as fractionation (Hubstenberger et al., 2017; Jain et al., 2016; Khong et al., 2017) or APEX coupled with proteomics and transcriptomics (Markmiller et al., 2018; Padron, Iwasaki, & Ingolia, 2019).

3.1 Fluorescence-assisted purification

A holistic and unbiased approach to identifying the composition of a biomolecular condensate is to purify them and analyse their protein and nucleic acids constituents. While fairly straight forward for large and stable condensates, such as the nucleolus

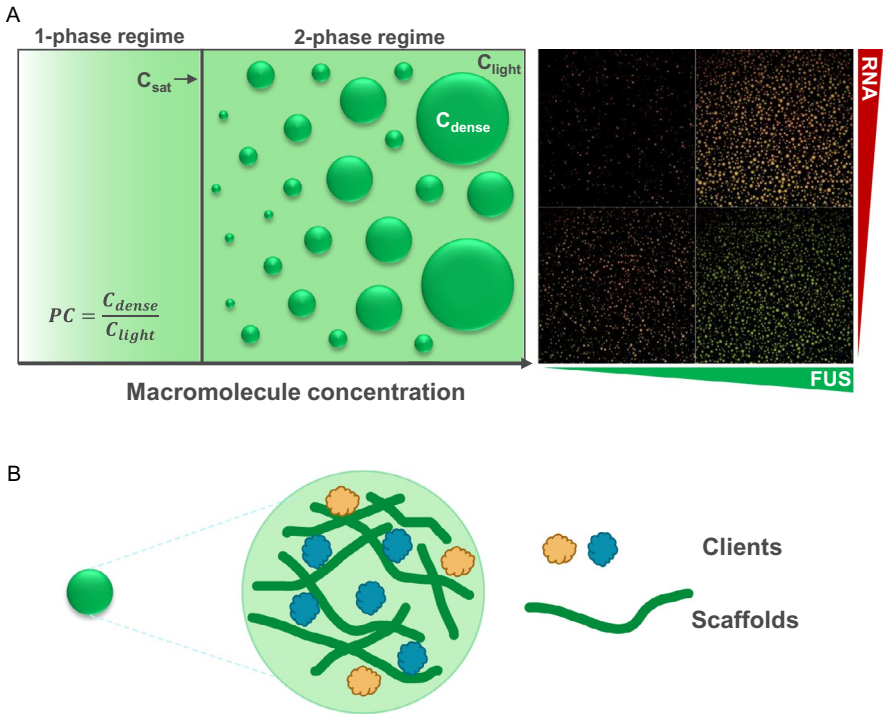

FIG. 4

Condensate composition. (A) Schematic representation of the progression of a macromolecule system from the 1-phase to 2-phase regime, as a function of concentration (left); Example of confocal microscopy images illustrating changes in composition and morphology of in vitro reconstituted condensates of FUS and RNA, fluorescently tagged with eGFP and Cy5, respectively. (B) Schematic representation of the scaffold network (green wavy lines), and recruitment of client molecules (clouds) in a multicomponent biomolecular condensate.

(Muramatsu & Onishi, 1978), efficient purification can prove challenging for condensates that are small and dynamic. For example, stress granules exhibit a two-layer architecture, with a stable core engulfed inside a labile shell (Jain et al., 2016). The stable cores are easily purified using a biochemical fractionation method, consisting of a series of centrifugation steps (Wheeler, Jain, Khong, & Parker, 2017); unfortunately, the shell is lost during the process (Jain et al., 2016). This purification of stress granule cores provides material of sufficient quality to perform proteomics (Jain et al., 2016) and transcriptomics (Khong et al., 2017) analyses. Hubstenberger et al. developed an ingenious adaptation of the classical biochemical fractionation, termed Fluorescence-Activated Particle Sorting (FAPS) (Hubstenberger et al., 2017). The method requires in-cell tagging of a biomolecular condensate marker,

with a fluorescent reporter. The cells are fractionated, and the fraction enriched in the condensate of interest, subjected to particle sorting by a fluorescence-assisted cell sorting instrument. The fluorescently labelled macromolecule is used as a reporter to follow the biomolecular condensates throughout fractionation, as well as a reporter in the particle sorting step. Hubstenberger et al. (2017)) utilized the FAPS technology to purify P-bodies from a HEK293 cell line expressing a GFP-tagged version of the LSM14A scaffold protein. The same workflow, however, could be used to purify P-bodies where the fluorescent reporter was bound to a nucleic acid component. The ability to sort the fluorescent biomolecular condensates using FAPS depends on their size and the limit of detection of the FACS instrument used. P-bodies, which were successfully sorted have an approximate diameter of ~500 nm (Hubstenberger et al., 2017), which pushes on the lower limits of FACS sorting technology.

Condensates that are more liquid in nature, as opposed to those with viscoelastic or gel-like material properties, present a challenge for FAPS, because they would deform and/or be destroyed due to the shear stress inside the flow sorter. Additional steps such as chemical crosslinking (Jain et al., 2016) which stabilize the labile interactions can be included in the protocol to make them robust enough for FAPS.

While elegant, there are several challenges and cautionary notes that researchers should consider when embarking on a condensate purification quest. First, it is imperative that the integrity of the purified particles is validated by comparing them against the composition, size and morphology of the condensate in the cellular setting, using orthogonal methods, such as IF and FISH.

3.2 Protein mapping

Once a marker protein for a condensate of interest has been determined, it is often useful to identify additional components of that condensate. A simple but effective way to do this is to image the condensate marker protein alongside a panel of candidate components using IF and/or other orthogonal labelling methods described above. If the fluorescence signal for the candidate protein appears enriched in the condensates where the target protein is enriched, the candidate protein is likely a component. An example of a protein showing enrichment of signal in a condensate by IF is shown in Fig. 5. In the figure, stress granule condensates are marked by the scaffold protein G3BP1, and an additional component of stress granules, eIF3, is visualized by IF and shows clear signal overlap within the stress granule.

Candidate proteins can be chosen based on previously known biology or identified through the unbiased omics methods mentioned previously. One limitation of conventional fluorescence-based mapping is that only a few proteins can be assayed at a time. A typical fluorescent microscope has the capacity to image up to four non-overlapping channels; more advanced microscopes are able to simultaneously separate up to six colours using the available four laser lines (Eissing et al., 2014). When imaging cells in a typical confocal microscope, one channel is usually claimed by a nuclear dye and one is needed to visualize the condensate marker protein, leaving

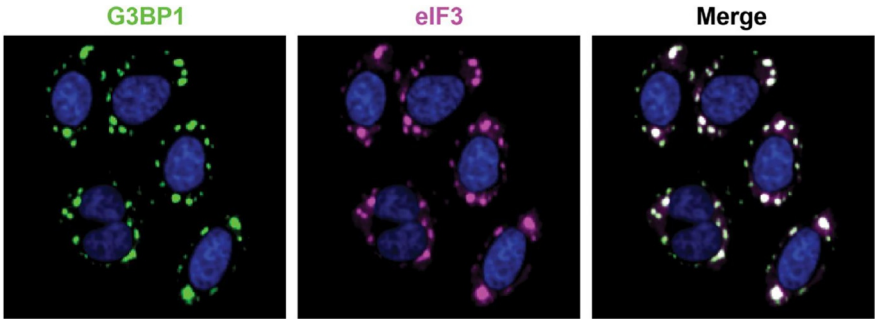

FIG. 5

Visualizing biomolecular condensates via immunofluorescence. Confocal fluorescence microscopy image showing co-localization of G3BP1 and eIF3 proteins in stress granules in HeLa cells. Images courtesy of Raffi Manoukian.

two additional channels available for monitoring candidate proteins. Because condensates can have hundreds of components, this necessitates visualizing many candidate proteins independently from one another. Additional insights, such as frequency and combinatorial analysis of co-localization could be obtained if it were possible to simultaneously monitor many components of a single condensate of interest, in the same cell sample.

The Pelkmans lab has recently developed an IF-based technique called "4i" (Gut, Herrmann, & Pelkmans, 2018). In 4i, up to ~40 proteins can be imaged in a single cell using multiple, sequential rounds of antibody staining, imaging, and washing (Fig. 6). Because the antibody is washed away after each round of imaging, the need for simultaneous multi-colour imaging capability is evaded. After all rounds of imaging are completed, images from each round can be superimposed. This high dimensionality of data allows the detection of subtle changes in condensate composition or cell state in response to stimuli such as cellular signals or drug treatments that would normally not be detected. Importantly, it provides insights into whether any one protein localizes to a single or to multiple types of condensates. Furthermore, the multiplexing power of 4i can help answer questions regarding the extent of compositional heterogeneity within the same family of condensates.

While powerful, 4i is a technically challenging technique that requires specialized equipment and analysis software. An additional consideration for both traditional IF and 4i is that certain commercial antibodies may not be specific to the advertised protein target, and thus all antibodies should be validated. One way to validate antibodies for IF is to perform staining on cells with the antibody target protein knocked down or knocked out and compare the staining to unperturbed cells (Uhlen et al., 2016). A specific antibody will show a decrease in the signal intensity proportional to a decrease of protein levels in the knockdown cells compared to the unperturbed cells (Uhlen et al., 2016).

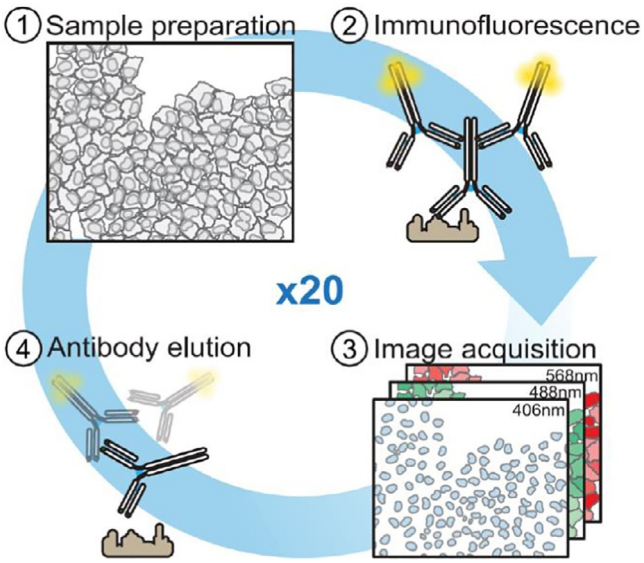

FIG. 6

4i technology for multiplexed immunofluorescence. Samples are fixed and immunostained with an unconjugated antibody of interest, followed by a fluorescently conjugated secondary antibody; fluorescence micrographs are acquired; the antibody complex is eluted and the process is repeated successively for tens of antibodies.

Image reproduced with permission from Gut, G., Herrmann, M.D., & Pelkmans, L. (2018). Multiplexed protein maps link subcellular organization to cellular states. Science, 361.

Similar to proteins, nucleic acids can be fluorescently labelled in cells or tissue via FISH, by taking advantage of the high affinity and specificity of nucleotide complementarity.

3.3 RNA mapping

FISH techniques have found multiple applications, from mapping the chromosomal structure, to understanding gene expression, and lately, to studying the composition and architecture of biomolecular condensates. For example, Fei et al. performed a quantitative analysis of the correlation between the degree of specific RNA incorporation within nuclear speckles and the size of the condensates using smFISH (Fei et al., 2017). Lee et al. utilized smFISH to map, in vivo, specific mRNA molecules identified by transcriptomics to be recruited to P-granules in *C. elegans* (Lee et al., 2020).

Typically, the procedure for hybridization requires fixation and permeabilization of the sample, to facilitate delivery of the fluorescent probe to the site of the nucleic acid of interest. These requirements pose a major challenge when needed to preserve the viability of the sample. Batani, Bayer, Boge, Hentschel, and Thomas (2019)

recently reported a procedure to hybridize RNA with fluorescent DNA probes in live bacteria. Furthermore, they took advantage of the fluorescent labelling to FACS sort the hybridized bacteria into different taxonomic pools. The possibilities of applying this emerging technique to the study of biomolecular condensates is intriguing.

3.4 Concentration and partition coefficients

The partition coefficient (ratio between the concentration within the dense phase versus the light phase; Fig. 4A) of a biomolecule is often utilized as a metric for assigning a macromolecule a scaffold versus client role in a condensate (Fig. 4B) (Banani et al., 2016; Xing et al., 2020), or as a metric of changes in the composition of a condensate (Banani et al., 2016; Ferrolino, Mitrea, Michael, & Kriwacki, 2018; Mitrea, Chandra, et al., 2018; Riback et al., 2020). The partition coefficient can be calculated from quantitative analysis of fluorescence microscopy images of cellular condensates in live or fixed cells, as well as in vitro reconstituted condensates (Mitrea, Cika, et al., 2018; Riback et al., 2020). Alternatively, the partition coefficient can be calculated in vitro, by physically separating the dense and the light phases and measuring their respective fluorescence (if a fluorescent probe is available on the target macromolecule), or their absorbance (Martin et al., 2020).

For fluorescence-based measurements of the partition coefficient, the molecule of interest must be tagged with a fluorescent probe. If using microscopy and quantitative image analysis (Banani et al., 2016; Ferrolino et al., 2018; Klein et al., 2020; Mitrea, Cika, et al., 2018; Riback et al., 2020; Xing et al., 2020), the respective fluorescence signal in the dense and light phases is integrated and used to calculate the partition coefficient.

In order to accurately correlate the fluorescence signal with the macromolecule concentration, it is imperative that the stoichiometry of fluorophore to macromolecule can be accurately determined. Chemical or genetic labelling are preferred, due to the fact that the stoichiometry and labelling efficiencies can be controlled, or at the least, properly measured. Due to potential variability in epitope accessibility in the context of a condensate versus the dilute phase, for the primary antibody, along with the unpredictable level of amplification generated by the secondary antibody, IF is not recommended as a quantitative measure for the partition coefficient.

The partition coefficient is a relative parameter. For certain applications, researchers need to determine the exact protein concentration of a target molecule inside and outside the condensate. For quantification of concentration inside NPM1 in vitro condensates (Ferrolino et al., 2018), and for the concentration of Fibrillarin inside nuclei of dividing *C. elegans* embryos (Weber & Brangwynne, 2015), this was achieved by building calibration curves with the fluorophore in solution, and interpolating the integrated fluorescence intensities of the dense phases.

The state-of-the-art method used in the field for quantitating the protein concentration in live or in vitro reconstituted condensates is fluorescence correlation spectroscopy (FCS). The fit of the FCS correlation curve returns a set of three key parameters: (1) fluorophore concentration, (2) brightness of the diffusing species,

which is a measure of the oligomerization state, and (3) diffusion coefficient. This approach was used to define the full phase diagrams of hnRNPA1 protein in vitro (Martin et al., 2020) and in transcriptional condensates in mammalian cells (Wei et al., 2020).

It is well understood that the crowding (Bancaud et al., 2009; Li et al., 2012), viscosity (Elbaum-Garfinkle et al., 2015), pH (Martin et al., 2015), and possibly other parameters of the dense phase are different compared to the light phase. Depending on the nature of the fluorophore used, either one or more of these differences could influence the quantum yield to different degrees (Mitrea, Cika, et al., 2018). Increased local concentration of the fluorophore inside the dense phase can also result in quenching of the fluorescence signal (Mitrea, Cika, et al., 2018; Morikawa et al., 2016). Consequently, any of these photophysical alterations induce non-linearity in the measured fluorescence intensity signal, producing inaccurate values for the partition coefficient. Therefore, caution should be exercised to minimize the impact of such effects. For example, the change in quantum yield due to viscosity can be measured, and corrected for, as described in Mitrea, Cika, et al. (2018). The effect of self-quenching of the fluorophore due to increased local concentration can be mitigated by spiking in a small amount of labelled material in an excess of unlabelled molecules (Elbaum-Garfinkle et al., 2015; Ferrolino et al., 2018; Mitrea, Cika, et al., 2018). While this approach is readily tractable in vitro, the effects of a fluorescent tag in vivo are more challenging to address.

Due to the compositional complexity of biomolecular condensates, and the dynamic nature of biological processes, the partition coefficients of individual components are constantly modulated. In the next section a discussion will be provided on how fluorescence-based techniques can provide insights into the discreet architecture of condensates and the dynamic features of their components.

4 Condensate morphology and dynamics

Biomolecular condensates have a complex composition, sometimes encompassing hundreds to thousands of components (Andersen et al., 2005; Hubstenberger et al., 2017; Jain et al., 2016). Along with this, often comes a complex architecture, with co-existing phases that compartmentalize specific components or function. For example, the nucleolus is a multilayered condensate which hosts and controls ribosome biogenesis, by compartmentalizing the different steps in the process: ribosome RNA synthesis, processing and assembly (reviewed in Boisvert, van Koningsbruggen, Navascues, & Lamond, 2007). By comparison, the nucleolus is one of the largest biomolecular condensates recognized to date, measuring up to ~1–2 μm in mammalian cells and ~20 μm in *Xenopus laevis* oocytes. Therefore, the three layers are readily detectible via conventional, diffraction limited fluorescence microscopy (Feric et al., 2016). Other condensates, however, are smaller, impinging on the diffraction limit, making their detection, and of any potential ultrastructural features, unable to be resolved by means of confocal fluorescence

microscopy. For example, transcriptional condensates proved particularly challenging to study by conventional imaging methods due to their small sizes, nearing the diffraction limit. To investigate their architecture, composition and dynamics during active transcription, state-of-the-art super resolution microscopy techniques were employed, as discussed in the following section.

4.1 Super resolution microscopy

Super resolution microscopy techniques include structured illumination microscopy (SIM), Stochastic Optical Reconstruction Microscopy (STORM)/Photoactivated Localization Microscopy (PALM) and Stimulated Emission Depletion (STED) microscopy (reviewed in Mitrea, Chandra, et al., 2018; Sydor, Czymmek, Puchner, & Mennella, 2015; Table 3), where the detection limit can reach as low as ~10–20 nm. The specifics of each method and how they compare to standard confocal microscopy are listed in Table 2. These super resolution techniques have a distinct advantage for analysing the architecture of small condensates.

An example of such a sub-micron condensate is the nuclear speckle. The layered ultrastructure of its protein components (i.e., SC35, SON) and RNA components (i.e., *MALAT1* and small nuclear RNAs), clustered towards the centre and periphery of the condensate, respectively, was detected using multi-colour SIM

Table 3 Comparison between conventional and super-resolution microscopy techniques.

Technique name	Resolution limit	Advantages	Disadvantages
Confocal	~200 nm	Live and fixed cell imaging Compatible with dynamics measurements Fast acquisition Low cost High throughput	Diffraction limited
2D/3D SIM	~100 nm	Live & fixed cell imaging Fast acquisition Improved resolution High throughput	High cost/specialized equipment Prone to reconstruction artefacts
PALM/ STORM	~10 nm	Best resolution Live and fixed cell imaging Compatible with dynamics measurements	High cost/specialized equipment Specialized dyes Slow acquisition Low throughput
STED	~10 nm	Best resolution Live and fixed cell imaging Compatible with dynamics measurements	High cost/specialized equipment Specialized dyes Slow acquisition Low throughput

(Fei et al., 2017). In bacteria, 3D SIM was employed to determine the ultrastructure of the transcribing nucleoid in live *E. coli*, based on a RNAP-GFP genetically encoded marker (Stracy et al., 2015).

In order to obtain even higher resolution data than that provided by SIM, single molecule-tracking using live cell PALM and a reporter photoactivatable mCherry fluorescent protein tag fused to the RNA polymerase, was applied to demonstrate that the *E. coli* nucleoid undergoes spatial reorganization in response to active transcription, in vivo (Stracy et al., 2015). Furthermore, Cho et al. used PALM and single molecule tracking of a Dendra2-tagged Mediator and RNA polymerase II in live embryonic stem cells, to quantify the residence time of active transcription clusters (Cho et al., 2018).

Super resolution techniques require specialized, photoactivatable fluorescent tags or dyes and specialized instrumentation. STORM/PALM and STED rely on the stochastic blinking of the fluorophore attached to the target of interest, to generate a precise mapping of its location. While superior at detecting static and dynamic features at the single molecule level, the super resolution techniques are slow compared to conventional microscopy. Thus, only dynamic processes that occur at time scales slower than the acquisition rate can be accurately captured. Live imaging is possible only if the samples are stable over the long course of the acquisition. Alternatively, it is advisable to fix the samples. The cost in time that comes with enhanced resolution is also not compatible with automation and high throughput features, which are typically achievable with conventional microscopy.

Collectively, imaging techniques, both conventional and super-resolution, coupled with mapping provide critical insights into the internal architecture, composition and dynamic features of biomolecular condensates. These features determine the material properties of these condensates; the methods used for their characterization will be discussed in the next section.

5 Material properties characterization

In addition to their unique architecture and complex composition, another important hallmark that emerges from the intricate interplay between proteins and nucleic acids within the dense phase of condensates, are highly-tuned material properties (Alberti, 2017; Wei et al., 2017). Specifically, in the context of disease, drastic changes in the material properties of biomolecular condensates were reported for various proteins and model systems (Alberti & Dormann, 2019; Patel et al., 2015; Shin & Brangwynne, 2017). Thus, a critical question is: how to effectively assess the material properties of biomolecular condensates? Tracking the dynamic behaviour of fluorescent markers inside biomolecular condensates, as well as measuring the bulk viscoelastic properties of condensates, provide insights into their material properties.

Before selecting a given technology, it is important to critically examine the pros and cons of performing measurements of material properties inside a living system versus a highly controlled environment such as in a reconstituted in vitro setting. In

contrast to a cellular scenario, where the condensates under study are typically surrounded by the plasma membrane, reconstituted condensates have the advantage of being directly accessible within the buffer. After an initial incubation time, the condensates sink to the coverslip surface and form static drops that can be easily imaged and assed with a variety of tools, as described below. Another advantage in such a setting is the precise control over most of the tunable parameters, such as selection and concentration of the macromolecule(s) of interest, salt, pH, temperature, etc. This precise control over the reconstituted system comes at the expense of the reduction in compositional, signalling and regulatory complexity, relative to the cellular setting. In the following section, the technologies will be reviewed that directly probe the material properties of condensates and discussion will be provided on their compatibility with measurements of in vitro reconstituted droplets and condensates formed in living cells.

Viscosity, surface tension and stiffness are the material properties that are most often characterized in the study of biomolecular condensates; these measurements frequently take advantage of fluorescently-labelled probes, as described below.

For highly viscous liquid condensates or gel-like aggregates, such as Huntingtin aggregates, atomic force microscopy (AFM) (Duim, Chen, Frydman, & Moerner, 2011) serves as a relevant approach to measure the stiffness of the materials by using a cantilever to probe along the surface of a particle, such as a cell or an isolated condensate. Louvet et al. used AFM to interrogate changes in the stiffness of purified nucleoli in response to stress stimuli, for example, inhibition of transcription and proteasomal degradation (Louvet, Yoshida, Kumeta, & Takeyasu, 2014). They validated the integrity and proper architectural organization using IF against markers of each of the three layers of the nucleolus (Louvet et al., 2014).

However, for very soft materials, AFM measurements can be significantly biased by wetting effects of the condensate with the cantilever and even the stiffness of the mounting surface can have significant effects on the derived material properties.

Viscosity and surface tension can be measured by tracking the signal of a visual marker (i.e., fluorescence or contrast) of the condensate of interest. For example, Brangwynne and colleagues described a method, termed inverse capillary velocity, which extracts the ratio between the viscosity and surface tension, by tracking the kinetics of fusion and relaxation of two coalescing condensates. This technique has been applied to nucleoli in *Xenopus laevis* oocytes (Brangwynne et al., 2011), as well as in in vitro reconstituted LAF-1 droplets (Elbaum-Garfinkle et al., 2015). In order to perform such fusion experiments in free solution in a highly controlled manner, optical tweezers have been successfully used to understand the tuning of material properties of condensates with respect to protein sequence (Patel et al., 2015; Wang et al., 2018). Notably, even though these measurements provided valuable insights, the procedure requires a dedicated and expensive optical tweezers setup, and a highly trained person to perform these tedious experiments. Catching a diffusing condensate is not easy. In order to increase the throughput and reduce the cost of such measurements, microfluidic chips provide a great potential to apply a deformation force by using hydrodynamic flow fields (Linsenmeier, Kopp, Stavrakis, de Mello, & Arosio, 2020; Shen et al., 2020).

As a cautionary note, reconstituted condensates will eventually interact with surfaces, which leads to changes in the material properties that are being measured. Passivating the surfaces with low-binding polymers, tested for the condensate of interest to ensure that wetting is prevented (i.e., PEG, Pluronic, Sigmacote, etc.) (Alberti et al., 2018; Feric et al., 2016), or using commercially available protein non-binding multi-well plates and/or slides reduce such side effects substantially.

Insights into material properties, such as viscosity and dynamic behaviour of target proteins inside the condensates, both in vitro and in live cells, can be obtained by live tracking of diffusing fluorescently labelled probes. These methods will be discussed in the following sections.

5.1 Fluorescence recovery after photobleaching

The most widely used approach to measure a change in material properties of condensates is fluorescence recovery after photobleaching (FRAP). FRAP can be readily applied to in vitro reconstituted, as well condensates inside living cells (Feric et al., 2016; Patel et al., 2015; Taylor, Wei, Stone, & Brangwynne, 2019; Woodruff et al., 2017). The technology relies on a strong laser beam that is focused into a fluorescently-labelled object, such as a condensate (Fig. 7A–B). Due to the high laser power, fluorophores inside the focal volume will be photobleached. The fluorescence signal (I_t) will recover if the photobleached molecules are replaced by fluorescent molecules diffusing into the space that was bleached. Therefore, the time needed for the photobleached region to recover its fluorescence signal (τ, recovery time) is a quantitative measure for the diffusion coefficient of the selectively-labelled component (Eq. 1). Furthermore, the amplitude of the recovery curve is a quantitative measure of the mobile fraction (M_f) of fluorescently labelled molecules (Eq. 1). For a more in-depth discussion on the analysis and interpretation of FRAP data, the reader is directed to Taylor et al. (2019).

$$I_t = M_f\left(1 - e^{-t/\tau}\right) \tag{1}$$

The diffusion rates and mobility of the marker molecule will depend on the viscoelastic properties of the condensate milieu, as well as the valency and strength of interactions inside the condensate. Therefore, the FRAP curves of scaffold and client proteins can differ significantly, even within the same condensate. For example, Woodruff et al. performed FRAP analysis on multiple components of the centrosome inside *C. elegans* embryos, as well as in in vitro reconstituted condensates and showed that SPD-5 has a very long recovery time potentially serving as a rigid scaffold, whereas other proteins such as PLK-1 recover much faster, likely serving as clients (Fig. 7C–F) (Woodruff et al., 2017). Components within liquid-like condensates will exhibit a full recovery to pre-bleached intensity and the diffusion coefficient can be extracted from the recovery time by fitting the data to a diffusion model. However, scaffolds within viscoelastic, gel-, or solid-like condensates might not

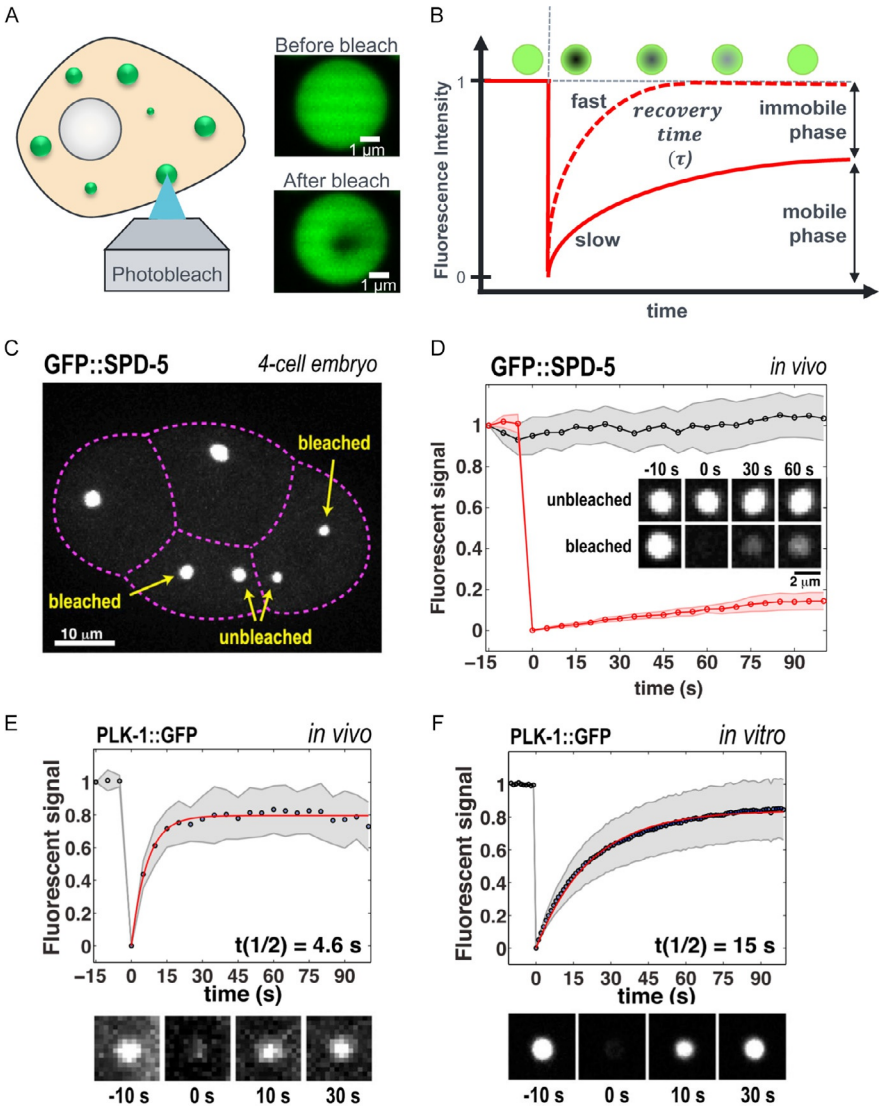

FIG. 7

Characterization of condensate material properties. (A) Schematic representation of FRAP; a highly-focused laser beam selectively bleaches a fluorescently-labelled protein inside a cell (left); fluorescence micrograph of an in vitro reconstituted FUS-eGFP condensate before (top) and after (bottom) partial photobleaching (dark spot in centre of condensate). (B) Model representation of fluorescence recovery curves for a highly mobile (dashed line) and a less mobile (continuous line) condensate component. (C) Centrosomes labelled by incorporation of genetically-encoded GFP::SPD-5 fusion protein. (D) FRAP curve of GFP::SPD-5 scaffold protein in centrosomes in vivo (red), compared to unbleached centrosomes control (black). FRAP recovery curves of the client centrosome protein PLK-1::GFP in vivo (E) and in vitro (F).

Panels (C–F): Reproduced with permission from Woodruff, J.B., Ferreira Gomes, B., Widlund, P.O., Mahamid, J., Honigmann, A., & Hyman, A.A. (2017). The centrosome is a selective condensate that nucleates microtubules by concentrating tubulin. Cell, 169, *1066–1077 e1010.*

recover according to a simple diffusional model; for such examples, care must be taken in interpreting molecular dynamics results (Zhu et al., 2019).

A more technical remark relates to the proper correction for global bleaching during the recording of the FRAP curves. The object that was bleached by the FRAP laser will be continuously illuminated by the imaging light source, causing an additional source of bleaching, which is experienced by the entire field of view. This effect can be detrimental for dimly-labelled condensates (i.e., low signal-to-noise ratio) inside live cells. If not corrected precisely, the recovery amplitude would be underestimated and therefore the condensate would be considered to be more "gel-like" even though the system might fully recover. Moreover, motion artefacts can bias the analysis significantly, if the condensate under study moves out of focus, causing an artificial decrease in signal. Hobson et al. describe selective plane illumination microscopy (SPIM) as a solution for correcting such motion artefacts, with applications in living embryos and live cells (Hobson, O'Brien 3rd, Falvo, & Superfine, 2020).

In summary, FRAP is a technology that is widely available and easily integrated into any conventional fluorescence microscope. Moreover, no special sample preparation is required, labelled proteins that are used for standard fluorescence live imaging can be also used for FRAP. The main limitations of FRAP, particularly when applied to condensates, is the size of an object to be photobleached. In order to probe the diffusion of molecules within the dense phase of the condensate, and avoid contributions from diffusion of molecules across the condensate interface, the photobleached region is typically small with respect to the size of the condensate, and positioned away from the interface (Fig. 7A). However, the focal volume of a well-aligned FRAP system using a high magnification objective lens (i.e., 60× NA 1.2 water immersion lens or 100× NA 1.35 silicone immersion lens) is in the range of about 0.7–1 μm. Therefore, objects with a similar size or even smaller than the bleach spot can only bleach completely. This makes the analysis much more tedious, due to the need to disentangle the multiple mechanisms that contribute to the fluorescence signal recovery. Towards this end, Taylor et al. developed a sophisticated 3D model to relate the diffusion coefficient D to the condensate radius with respect to the bleach spot size (Taylor et al., 2019). FRAP is instrumental in determining relative changes, such as identifying material properties or dynamic differences between wild-type and mutant, or between untreated and drug-treated condensates. However, determining absolute physical parameters such as viscosity, by monitoring FRAP of a condensate component remains still challenging due to multiple assumptions that are made in the process. Viscosity of a condensate, however, can be accurately determined using orthogonal microrheology methods, described next.

5.2 Microrheology

Microrheology can be used to measure the viscosity inside a condensate by tracking a fluorescent reporter that does not interact with the condensate milieu, but rather only senses its bulk viscosity. It is based on the principle of the Stokes-Einstein equation

(Eq. 2), which dictates that the diffusion (D) of a particle with a known hydrodynamic radius (R_h) which undergoes Brownian motion within a fluid, at temperature T, is inversely proportional with the fluid's viscosity (η):

$$D = \frac{k_B T}{6\pi\eta R_h} \tag{2}$$

Experimentally, fluorescent particles are introduced in a sample containing the microenvironment whose viscosity is to be measured (i.e., in vitro reconstituted droplets, live cells, living animals) and the trajectories of the particles inside the condensate are monitored via time-lapse fluorescence microscopy imaging. The diffusion coefficient is derived from the correlation between the mean-squared-displacement and time (Delarue et al., 2018; Elbaum-Garfinkle et al., 2015). Such reporters can be commercially-available fluorescent beads, which were used to measure the viscosity of LAF-1:RNA (Elbaum-Garfinkle et al., 2015) and nucleolus-like (Feric et al., 2016) in vitro reconstituted condensates. Delarue et al. utilized genetically-encoded multimeric fluorescence nanoparticles to measure changes in viscosity in live cells; by single-molecule tracking, they determined diffusion coefficients and derived the viscosity of the cytoplasm in the presence and absence of chemical treatment (Delarue et al., 2018).

In order to collect high quality data, a fluorescence microscope with rapid sampling capabilities, such as a spinning disk is needed. For accurate correlation between diffusion coefficient and viscosity of the microenvironment, it is crucial that the size and shape of the tracking fluorescent particle is homogenous and well-defined, and that the tracking particles do not interact with their microenvironment. Specific considerations when selecting commercial tracking beads, should be taken to ensure that the surface of the particle is compatible with, and interaction inert with the microenvironment inside the condensate. A surface that is incompatible with the condensate will cause the tracking bead to be excluded from the condensate. A surface that interacts with the condensate will cause the tracking bead to diffuse anomalously (Elbaum-Garfinkle et al., 2015). Furthermore, the size of the tracking beads must be chosen such that they report on the bulk viscosity of the condensate and are small relative to the size of the condensates, to allow tracking of Brownian motion inside the condensate. In order for a molecule or tracking particle to sense the bulk viscosity, its size must be larger than the mesh size—the threshold at which condensate properties impact molecular diffusion and permeability of a molecule or tracking particle (Wei et al., 2017).

A particular challenge for applying microrheology methods in living cells or organisms, is the delivery of the tracking particle to the correct location. To circumvent this, genetically encoded μNS virus tracer particles emerged as an elegant approach to deliver the tracer particle inside the cell (Munder et al., 2016). By tracking of those μNS particles followed by mean-square displacement analysis of the obtained particle traces, Munder and co-workers showed that the cytoplasm of yeast cells transitions into a solid-like state, by this effectively surviving harsh starvation

conditions. Collectively, these methods describe a passive microrheology approach (Fig. 8A), which allows approximation of viscoelastic properties of the material under study by carefully choosing the appropriate model systems (reviewed in Zia, 2018).

However, in order to obtain frequency-dependent and even non-linear response properties, the system must be driven out of equilibrium. For such active microrheology experiments the tracer is displaced by an oscillatory force, for example by magnetic (Bausch, Ziemann, Boulbitch, Jacobson, & Sackmann, 1998) or optical forces (Jawerth et al., 2018) (Fig. 8A). Jawerth et al. used this novel method based on optical traps to study the frequency-dependent rheology of P-granule protein PGL-3 condensates as a function of salt concentration (Jawerth et al., 2018). Specifically, as the salt concentration is reduced, the elastic modulus, viscosity, and surface tension increased for this type of condensate, a very valuable insight that could not have been obtained by using passive microrheology approaches.

A unique approach called focused-light-induced cytoplasmic streaming (FLUCS) (Mittasch et al., 2018) was utilized to measure material properties of biomolecular condensates (Mittasch et al., 2020) by using laser-induced hydrodynamic flows inside the cytoplasm of living embryos (Fig. 8B). Mittasch et al. (2020) found that throughout the cell cycle of the developing embryo the mechanical properties of the centrosome are highly tuned, undergoing a rapid transition from microtubule force resisting state to a weak, brittle conformation in anaphase. Interestingly, the observed material property transition is strongly correlated with the partition characteristics of client proteins such as PLK-1, SPD-2, and PP2A, suggesting that a well-tuned balance of the activities of such proteins determines the assembly/disassembly state of the centrosomal matrix. While FLUCS measurements allow for localized and precise mechanical force applications, the technology is not commercially available and therefore was implemented from scratch; a substantial amount of work went into constructing a device that will avoid undesired temperature effects and designing custom software for data acquisition and analysis.

5.3 Fluorescence correlation spectroscopy

In order to explore more deeply the quantitative biophysical analysis of condensates, Wei et al. (2017) developed a method based on FCS to measure concentrations and construct entire binodals, termed ultrafast scanning FCS (usFCS). They applied usFCS to LAF-1 and its intrinsically disordered RGG domain in the presence and absence of RNA molecules to determine the mesh size (~3–8 nm) for reconstituted and intra-cellular LAF-1 condensates. Compared to the previously discussed technology FRAP, usFCS requires highly dedicated hardware consisting of a special TAG lens, which allows to perform scan frequencies up 70 kHz. The calibration of such a custom-built device requires well established routines and controls as well as the willingness to develop software and hardware.

Another emerging technology to optically visualize a change of intracellular material properties is fluorescence lifetime imaging (FLIM). Laine et al. showed that

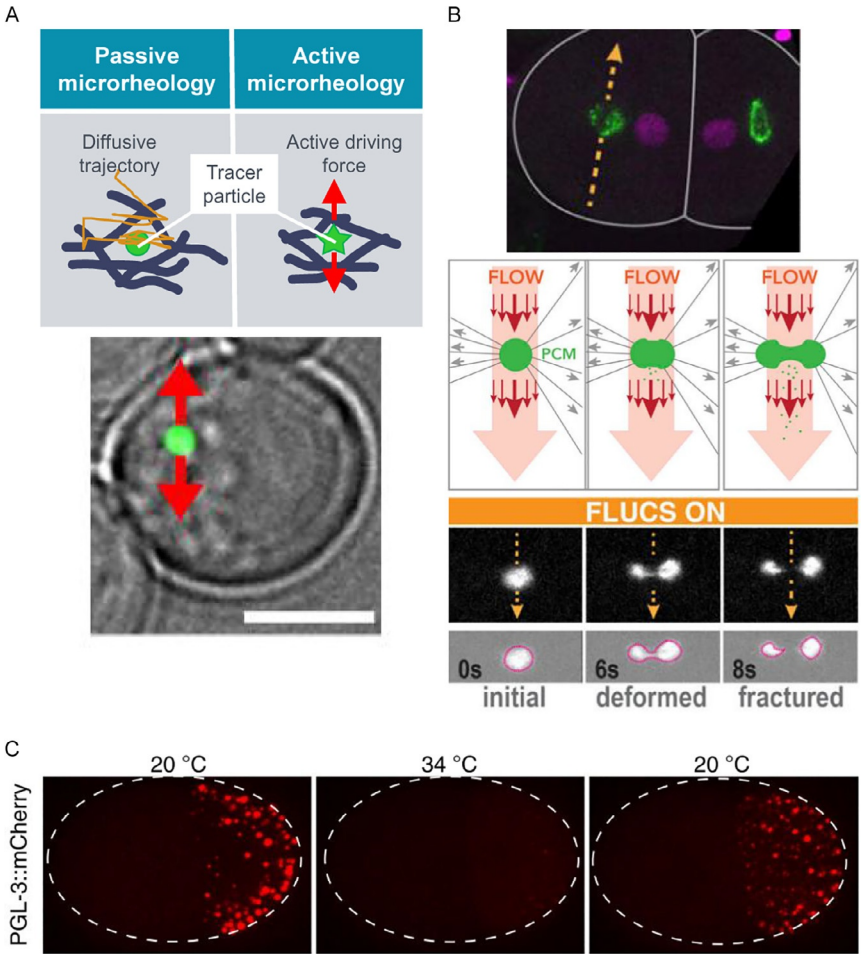

FIG. 8

Microrheology and active perturbations to determine material properties of condensates. (A) (Top) Schematic illustrating the difference between microrheology modes inside a densely condensed protein meshwork (blue lines). Passive microrheology tracks tracer particles undergoing Brownian motion (indicated by gold squiggle lines) and active tracks tracer particles actively displaced by an external force (indicated by red arrows). (Bottom) Micrograph of a living yeast cell with a genetically encoded fluorescent tracer particle subjected to active displacement; (B) (top and bottom) Highly localized laser-induced hydrodynamic flows are used to deform and eventually rupture condensates inside living *C. elegans* embryos (yellow dotted arrows indicate the localization and direction of the induced flow field). (Middle) Schematic illustrating hydrodynamic flows (red arrows) that cause a weakening of the pericentriolar material (PCM). Microtubule pulling forces are depicted by grey lines and arrows. (Bottom) A series of dynamic fluorescence images showing

a dedicated version of so-called time-gated FLIM can be used effectively to dissect the molecular mechanism of aggregation for amyloidogenic proteins such as α-Synuclein in vitro, in live cells and in *C. elegans* in live animals (Laine et al., 2019). Specifically, they demonstrated that the change in material properties is strongly connected to the degree of protein aggregation, which correlates with a decrease in the lifetime of the reporter fluorophore. FLIM has a higher throughput compared to FRAP and provides information about the aggregation states and their distribution of all the inclusions detected in the field of view in a single acquisition. Due to the non-destructive nature of FLIM, a developing or aging animal can be probed throughout a longer time course. However, FLIM might not be able to detect material property changes for fluid-like systems, since the well detectable decrease in lifetime is thought to be associated with strong amyloid fibrils formation, which is a very strong transition and therefore only applicable for a small subset of aberrant condensates.

As an alternative approach to fluorescence-based methods, stimulated Raman microscopy emerged as a powerful tool to detect the formation of aggregates inside living cells (Picardi et al., 2018). In contrast to fluorescence microscopy, Raman approaches utilize the interaction of electromagnetic radiation with a vibrating molecule, leading to elastically (Rayleigh scattering) and inelastically scattered light (Raman scattering). To overcome the low signal levels of spontaneous Raman, stimulated Raman microscopy uses two co-aligned incident beams to tune the excitation frequency exactly matching the resonance frequency of the molecule under study. While stimulated Raman microscopy still suffers from inherently weak signal-to-noise ratio, it provides the potential for label-free measurements due to well-known spectroscopic fingerprints, as for example PolyQ aggregates (Miao & Wei, 2020).

FIG. 8—Cont'd

the deformation and ultimate fracture of centrosome as a consequence of induced shear flow. The red circle indicates the shape of the centrosome; the diameter was used to measure the force resistance of the material; (C) Fluorescence micrograph of a living *C. elegans* embryo with polarized germ line granules (PGL-3::mCherry) showing reversible dissolution upon temperature increase from 20 to 37 °C.

Panel (A): Reproduced with permission from Mittasch, M., Gross, P., Nestler, M., Fritsch, A.W., Iserman, C., Kar, M., et al. (2018). Non-invasive perturbations of intracellular flow reveal physical principles of cell organization. Nature Cell Biology, 20, *344–351; Panel (B): Reproduced with permission from Mittasch, M., Tran, V.M., Rios, M.U., Fritsch, A.W., Enos, S.J., Ferreira Gomes, B., et al. (2020). Regulated changes in material properties underlie centrosome disassembly during mitotic exit.* The Journal of Cell Biology, 219; *Panel (C): Reproduced with permission from Putnam, A., Cassani, M., Smith, J., & Seydoux, G. (2019). A gel phase promotes condensation of liquid P granules in Caenorhabditis elegans embryos.* Nature Structural & Molecular Biology, 26, *220–226.*

6 Methods to control formation and dissolution of condensates

Biomolecular condensates are environmentally responsive compartments that form in live cells via phase separation, and their sizes cover ranges that are below and above the light diffraction limit. This means that a number of condensate types are not amenable to the morphological and biophysical characterization techniques described above, due to the fact that they are not readily detectable by conventional light microscopy. To overcome this limitation, several techniques have been developed, which allow formation of large condensates at a specified location within the cell and/or in response to an extraneous trigger. In the following paragraphs, methods will be discussed which enable tightly-controlled formation and dissolution of condensates at a particular location and time, as well as methods for global induction and disruption of condensates.

6.1 Global disruption and induction of condensates

Strom et al. (2017) have shown that inside the nucleus of living *Drosophila* embryos the application of a dedicated chemical species such as the aliphatic alcohol 1,6-hexanediol can be used to probe the material properties of phase-separated heterochromatin regions by globally disrupting weak hydrophobic interactions. As a cautionary note, while the effects of 1,6-hexanediol can be interpreted straightforwardly in vitro, the effects observed in dissolution of condensates in living cells can be confounded with the known toxic effects of the treatment (Kroschwald, Maharana, & Alberti, 2017). Towards this end, Putnam et al. used a similar approach to characterize the material state of germline granules inside living *C. elegans* embryos (Putnam, Cassani, Smith, & Seydoux, 2019). For this, the embryos were mounted in various buffer conditions (e.g., increasing salt concentration); by application of a short laser pulse, the rigid egg shell was disrupted and the cell interior was rapidly pushed out into the surrounding buffer (Fig. 8C). By analysing how rapidly different components of these complex germline granules dissolve provides another possibility to distinguish between a fluid-like (rapidly dissolving in high salt) and gel-like state (don't dissolve in high salt). Moreover, by exposing the embryo to drastic temperature changes, a dissolution of the fluid components of the granules was shown, whereas the gel-like potentially scaffold structures remained mainly unaffected by the temperature increase. One general remark when working with heat is to apply the temperature perturbation as quickly as possible in order to obtain the direct response of the material (e.g., dissolution) and not a heat-induced stress response of the cell.

Stress granules are cytoplasmic condensates that contain RNA, RNA binding proteins and translation factors (Mahboubi & Stochaj, 2017). Multiple types of stress stimuli, as well as chemical treatment with compounds that cause oxidative stress, modulate translation, proteasome inhibitors and ER stressors, can induce the

formation of stress granule formation. For example, Jain et al. used oxidative stress via sodium arsenite treatment to induce stress granule formation and assay the molecular composition of stress granules by proteomics (Jain et al., 2016).

6.2 Controlled induction of condensates

6.2.1 Chemically-induced dimerization

Multivalent interactions drive phase separation (Alberti, Gladfelter, & Mittag, 2019). One can artificially enhance the rate at which these interactions occur by altering the oligomerization state of a protein. Specific compounds can induce the dimerization of specific combinations of proteins, for example rapamycin, which induces dimerization of FKBP12 and FRB (Cermakova & Hodges, 2018). Many other methods have been reported to induce heterodimerization of proteins, which include dimerization of eDHFR- and HaloTag (Fig. 3D) enzyme-fused proteins in the presence of TMP (Fig. 3E) linked to HaloTag ligand. Zhang et al. devised a method to induce ALT-associated promyelocytic leukaemia nuclear bodies (APB) formation using this type of dimerization induction (Zhang et al., 2020). APB is a type of condensate associated with DNA damage repair factors and telomere components. They fused a SIM domain to eDHFR and the telomere protein TRF1 to Halo-enzyme. In the presence of TMP linked to HaloTag-ligand they were able to artificially generate APB condensates in the absence of DNA damage. This enabled them to probe scaffold/client relationships between different APB components and assess the functional consequence of condensation (i.e., telomere clustering).

6.2.2 Optogenetics

Optogenetic methods utilize engineered proteins that contain domains which undergo changes in response to light activation. One family of optogenetic designs replaces the oligomerization domain of a phase separation-prone protein of a condensate scaffold molecule with a photoactivatable domain, which are fused in frame with a fluorescent protein reporter. This oligomerization induces phase transition at the site of illumination. Several variations have been described by the Brangwynne lab thus far (Fig. 9). The OptoDroplets design fuses the dimerization domain of the photoactivatable Cry2 protein to the intrinsically disordered region (IDR) of a phase separation-prone protein. Photoactivation with blue light induces spatially-controlled and reversible formation of condensates in living cells (Shin et al., 2017). Droplets are formed when the light stimulus is applied, and dissolve when removed. A second design, termed Corelets, uses a two-element modular design, which forms a multivalent core and acts as a seed which recruits phase separation-prone IDRs in response to blue light activation. The technique offers the advantage for tuning the concentration at which phase separation occurs (Bracha et al., 2018). A third design, CasDrop, uses a four-elements modular design, where a catalytically inert Cas9 fusion localizes to a genomic locus specified by a guide RNA. The fusion recruits a phase separation-prone IDR via the photoactivatable dimerization domain used in the Corelets design (Shin et al., 2018). This technique provides the advantage of driving formation of, and anchoring condensates at a

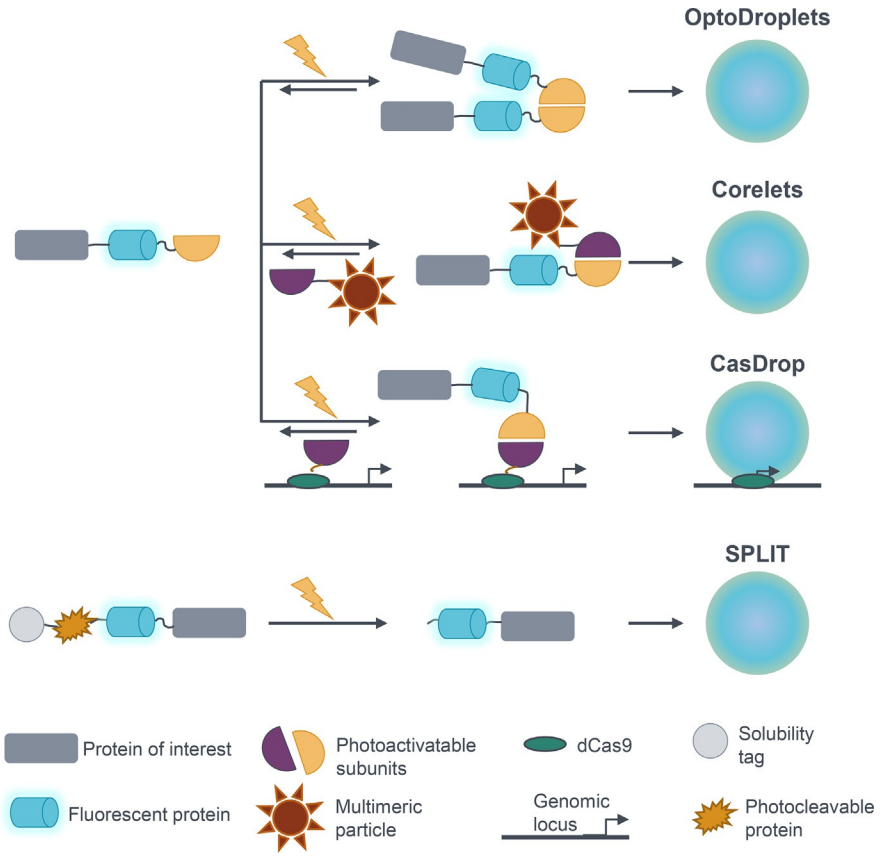

FIG. 9

Optogenetic methods for controlled formation of biomolecular condensates. Light-activated oligomerization designs: (A) OptoDroplets (Shin et al., 2017); (B) Corelets (Bracha et al., 2018); (C) CasDrop (Shin et al., 2018); Light-activated cleavage of a solubility tag (D) SPLIT (Reed, Schuster, Good, & Hammer, 2020).

well-defined, endogenous genomic locus. These three methods have the advantage of spatially and temporally controlling the formation of condensates and are compatible with live cell applications. The induction of condensates is reversible, which can be an advantage or disadvantage, depending on the desired application.

An alternative approach for induction of condensates, in a non-reversible manner is SPLIT (Reed et al., 2020), a design which fuses a photocleavable solubility tag to a fluorescent reporter and a phase separation-prone protein. This approach was successfully applied to induce condensate formation in response to short-term illumination at 405 nm in vitro and in *S. cerevisiae*.

6.2.3 Operon repeat arrays

Another system that allows for the controlled formation of condensates is the Lac array system, which is particularly useful when studying chromatin associated condensates such as transcriptional or heterochromatin condensates. In this system, a protein of interest (often an IDR) is fused to a fluorescent protein and the lac repressor protein, LacI and then expressed in cells harbouring a synthetic Lac operator (LacO) array. The LacI domains of the fusion proteins specifically bind to the LacO genomic repeats, thus increasing the local concentration of the protein of interest at that genomic site. If the protein of interest is capable of phase separation, this increase in concentration can promote condensate formation (Fig. 9A). While multiple Lac array cell lines exist, all recent studies utilizing this system (Boija et al., 2018; Chong et al., 2018; Klein et al., 2020; Zamudio et al., 2019) used a line containing ~50,000 LacI binding sites (Janicki et al., 2004). It should be noted that this line was not originally created to study condensates and thus the LacO repeats in these cells are interspersed with a number of other sequence features not used in the condensate studies.

The main advantage of the LacO array system is that it results in the formation of large condensates at a well-defined, albeit artificial, genomic locus that can easily be imaged with a simple confocal microscope. This is especially useful in the field of transcription where most endogenous condensates are sub-micron scale, and not readily detectable by diffraction-limited microscopy. One useful application of the LacO system is to test whether IDR-containing proteins form condensates and study the effects of mutations. An example showing a condensate forming protein compared to a non-condensate forming mutant version can be seen in Fig. 10B. The system has also been used to map what other proteins partition into condensates created by the LacI-tethered protein in mammalian cells (Boija et al., 2018; Chong et al., 2018; Zamudio et al., 2019), and bacteria (Ladouceur et al., 2020). These types of colocalization studies are very easy to perform on the large LacO array associated condensates.

While useful, the LacO array system is not a perfect model for endogenous condensates and certain precautions should be taken when interpreting results. First, seeing puncta in this system does not indicate a condensate has formed, because even without condensate formation many fluorescent proteins are tethered to the LacO array (Fig. 9B). To confirm there is a condensate, one should look for larger than average puncta compared to the control, fast FRAP recovery time (Fig. 7A–B) of the presumed condensate puncta, and in some cases, a difference in the refractive index inside versus outside the puncta (Chong et al., 2018). Finally, because the system relies on fusion proteins and the high repeat synthetic array, the composition and material properties of the induced condensates may differ from that of endogenous condensates. Thus, results obtained from these types of assays need to be rigorously analysed by considering all possible technique-related artefacts, and ideally any conclusions should be supported by orthogonal methods.

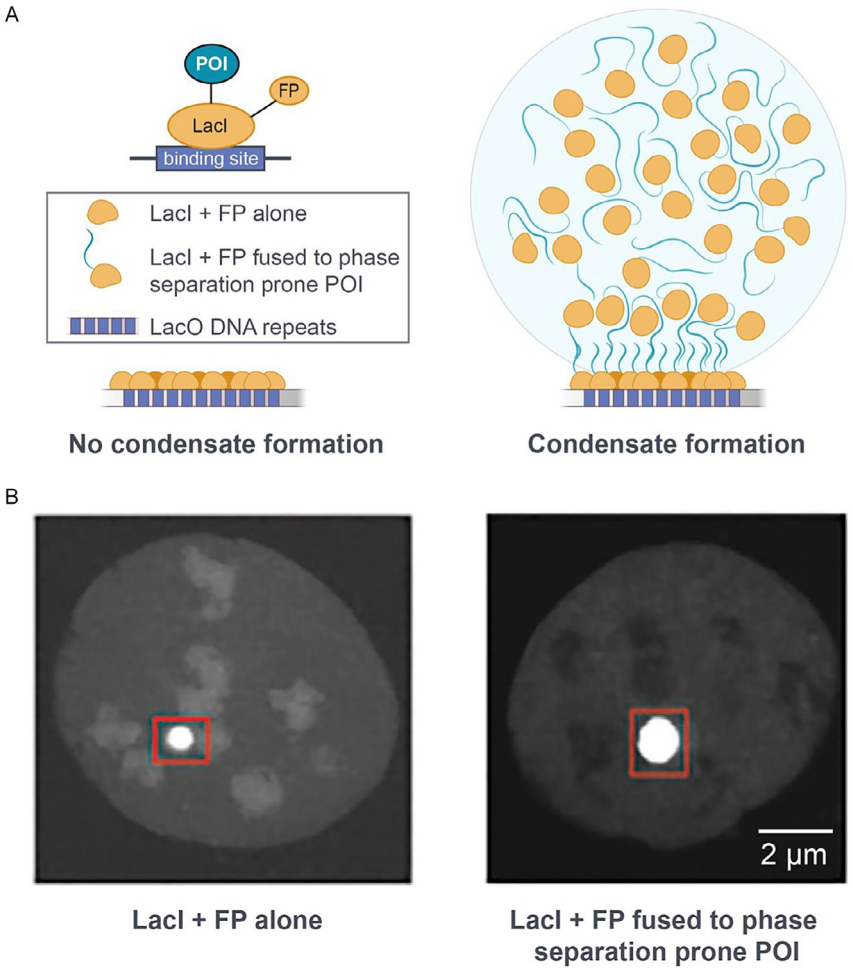

FIG. 10

Lac array model system for controlled formation of condensates in living cells. (A) Schematic representation of the LacO array locus and multivalent recruitment of the protein of interest (POI) and LacI conjugated to fluorescent protein (FP); (B) Example of in-cell induced CFP-GCN4 transcriptional condensates.

Image reproduced with permission from Boija, A., Klein, I.A., Sabari, B.R., Dall'Agnese, A., Coffey, E.L., Zamudio, A.V., et al. (2018). Transcription factors activate genes through the phase-separation capacity of their activation domains. Cell, 175, *1842–1855 e1816.*

7 Condensate phenotype in drug discovery

Condensates form upon certain stimuli such as cellular stress. They are transient, and reversible. They help the cells cope and adapt to a changed environment and are dissipated once the cells return to physiological conditions. However, if these

condensates are not dissipated, they tend to become toxic and pathological. This is often due to the change in material state of the condensate from transient liquid-like or gel-like state to a more solid-like state, a process called aberrant phase transition. Aberrant phase transitions are a hallmark of age-related diseases, like neurodegeneration (Fig. 11A). Several disease mechanisms can be attributed to the aberrant phase transition driven pathology of condensates (Fig. 11B). First, they can sequester

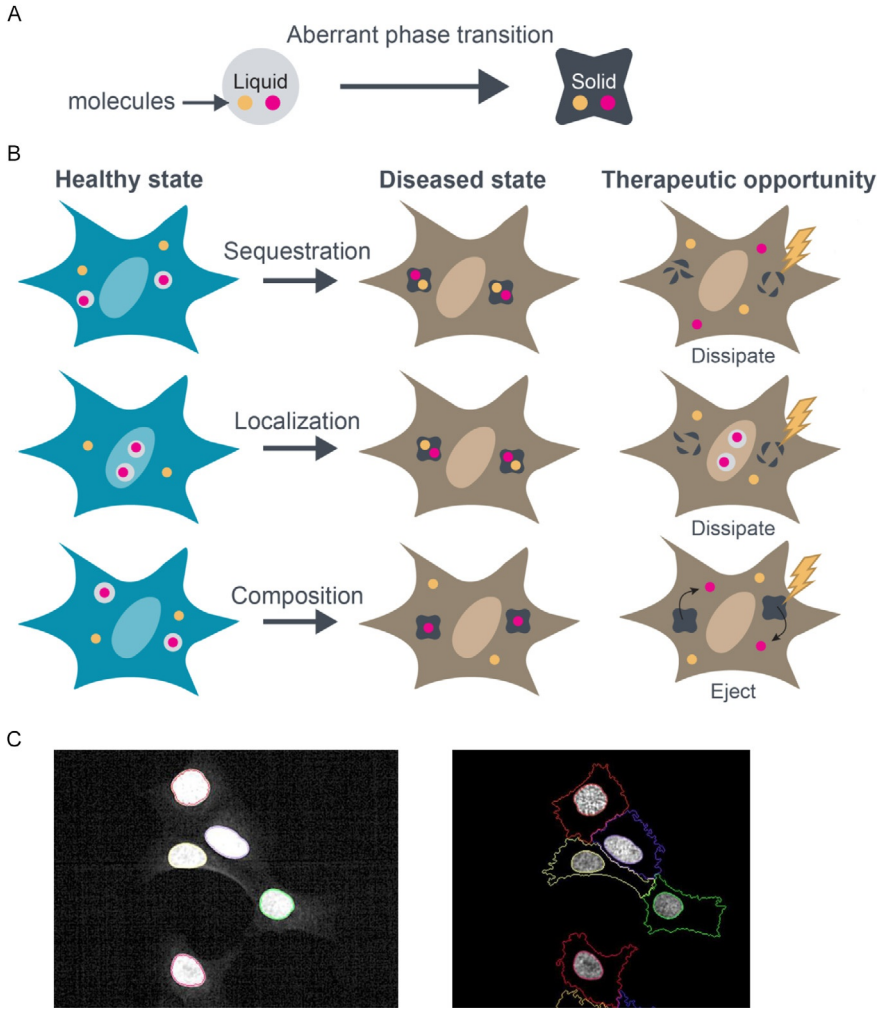

FIG. 11

Condensate-targeted drug discovery. (A) Aberrant phase transition; (B) Condensate-targeted opportunities for drug development; (C) Example of image segmentation of nuclei (left) and cytoplasm (right).

Images courtesy of Raffi Manoukian.

cellular factors that are responsible for cellular homeostasis. Second, they can mislocalize the molecules, leading to an associated gain or loss in function. Third, they can alter the physiological composition of the condensates. In all these cases, condensates are the precursor to a pathological state of the cell. Therefore, discovering small molecules that can target the condensate associated disease mechanisms have become quite attractive to design novel ways of treating such difficult to treat age-related diseases. Such therapeutic approaches include dissolution of aberrant condensates or selective ejection of proteins incorrectly localized to condensates (Fig. 11B).

Fused in Sarcoma (FUS) aggregates are a hallmark of Amyotrophic Lateral Sclerosis (ALS). FUS-containing stress granules form upon cellular stress and have liquid-like properties. Using purified recombinant proteins, it has been shown that liquid-like condensates undergo a liquid-to-solid aberrant phase transition that is accelerated by disease-linked mutations. Therefore, stress granules are thought to serve as compartments that can nucleate the pathological FUS aggregates. Wheeler et al. performed a compound screen to identify molecules that can dissolve or decrease the number of FUS-containing stress granules in human cells (Wheeler et al., 2019). They identified two compounds, Lipoamide and Lipoic acid, which were also able to rescue ALS-related phenotypes in animal models such as *C. elegans* and Drosophila. Similar studies for affecting condensates have been recently performed for the transcription factor p53. Strikingly, the small molecules that dissolve certain p53 mutant condensates were found to trigger the formation of condensates of certain other p53 mutants. This indicates that the same class of small molecules can differently affect the condensation behaviour of p53 mutant proteins (Lemos et al., 2020).

To identify promising compounds that affect the condensate phenotype, the marker protein for the condensate of interest is genetically tagged with a fluorescent protein, or fluorescently labelled via IF. In the following section, considerations will be discussed for the design, analysis and interpretation of phenotypic assays for condensate-targeted drug discovery.

7.1 Quantitative image analysis

As with any type of experiment, in the design phase of a condensate-based phenotypic assay, a number of parameters need to be optimized to ensure that the collected images are of the highest quality, and therefore lead to accurate image analysis results. In general, such considerations include selection and optimization of cellular density, type and number of cell type(s), controls, labelling methods for the target molecule(s), timing, live or fixed detection, etc. All these parameters must be optimized in order to facilitate accurate and reproducible image segmentation.

7.1.1 Image segmentation

Segmentation, which is the process by which the digital image is divided into multiple regions or segments, is the most important step in image analysis. In condensate-based phenotypic assays the interest is in segmenting three different regions: the cell

nucleus (Fig. 11C, left), the cell cytoplasm (Fig. 11C, right), as well as the condensates of interest. Segmentation of each region of interest is performed based on its own fluorescent marker.

Cell density is an important factor to properly segment the cells. An overcrowded field of view will give rise to an overlap with neighbouring cells, causing quantification artefacts. Too low a cell density will require acquisition of more fields of view to obtain significant statistical values, and therefore add to the acquisition time. This can be detrimental, especially when collecting live cell data.

The segmentation of the condensates relies on genetically-encoded fluorescent tags or IF signal. The biological controls need to provide a difference in the objects of interest, in this case, a phenotypic difference in the condensates. That difference can be absence versus presence of condensates, different localization of condensates between the controls, or significantly different intensities or sizes of condensates (Fig. 11B). Notably, the segmentation should be tested in the different controls before applying to the batch analysis pipeline, in order to establish an upper and lower threshold, and ensure that that the algorithm will correctly segment the full spectrum of phenotypes of the biological samples.

7.1.2 Quantification

In order to quantify the phenotypic difference between a treated and untreated sample, the following parameters can be quantified:

- *Cell number* is retrieved by counting the number of segmented nuclei using the DAPI/Hoechst channel. From this measurement cell toxicity can be inferred.
- *Intensity of the protein of interest in the nucleus* provides a proxy of the concentration of diffused protein of interest localized in the nucleus, as segmented based on the nuclear mask fluorescence signal.
- *Intensity of the protein of interest in the cytoplasm* provides a proxy of the concentration of protein of interest localized in the cytoplasm, as segmented based on the cytoplasmic stain fluorescence signal.
- *Intensity and area of the protein of interest in the condensates in nucleus and cytoplasm* provides a proxy of the total amount of protein inside the condensates, in the cellular compartment of interest, segmented as described above.
- *Intensity of the protein of interest outside the condensates* is a proxy for the concentration of the light phase. This value is obtained from the inverted mask of the condensates within the segmented compartment of interest (i.e., nucleus or cytoplasm).
- *Condensate shape* can be used to detect morphological changes (i.e., aggregation) by quantifying the roundness of the condensate.

When monitoring more than one protein, (i.e., more than one fluorophore), and therefore using more than one channel, the possibility for emission light bleed-through between channels should also be considered. This contribution should be corrected for when analysing the images. The bleed-through signal can be obtained by using samples that only contain one of the fluorophores of interest and acquire both

channels. The signal obtained in the channel corresponding to the omitted fluorophore represents the bleed-through signal and should be subtracted from the multi-colour image.

Moreover, when using antibody staining it is also good practice to have samples where the antibody should not bind, in order to control for "unspecific binding"; this signal should also be subtracted in the analysis.

Recruitment measurements and co-localization assays are used to determine recruitment and co-localization of macromolecules of interest within a condensate of interest. For example, in order to determine if protein A and B co-localize to the same condensate, the condensates are segmented based on the fluorescence signal of protein A, and the intensity of protein B inside the resulting mask is quantified. Relative stoichiometric ratios and partition coefficients can be derived from such measurements. In order to avoid artefacts caused by signal overlap in the XY plane, but originating from different Z planes, it is advisable to generate Z-stacks and confirm the co-localization in a 3-dimensional reconstruction. The acquisition of Z-stacks is more time consuming and increases the complexity of the analysis.

7.1.3 Live cell imaging

Live cell imaging allows for monitoring of fusion events, determining mobility between molecules (using FRAP) and measuring changes such as growth or aging of a condensate over time. The segmentation and quantitative image analysis described above will be applied for each time frame to monitor time-dependent changes in the condensates. Tracking algorithms can be employed to monitor time-dependent effects for individual condensates.

One of the considerations to keep in mind when performing live cell imaging is photobleaching, due to long-term exposure to the excitation light. As discussed in Section 5.1, this effect should be minimized, and if possible, corrected for in the analysis step.

These practical considerations are instrumental in the identification of drug candidates that modulate the condensate phenotype and composition in living cells. Intriguingly, the mechanisms by which small molecules interact and impact condensates are not fully understood. In the following section, new insights are discussed which connect the ability of a small molecule to accumulate within a biomolecular condensate with its therapeutic efficacy.

7.2 Drug partitioning into condensates as a consideration to drug efficacy

Drugs have been shown to selectively concentrate in biomolecular condensates. Klein et al. showed that specific small molecules (i.e., anti-cancer therapeutics) concentrate in condensates with different macromolecular composition through a series of biochemical and cell-based assays (Klein et al., 2020). Using an in vitro droplet reconstitution system, they demonstrated that cisplatin, tamoxifen and THZ1 concentrate in MED1 condensates, but not BRD4, SRSF2, HP1α, FIB1 or NPM1 condensates. These purified proteins represent different nuclear condensates associated

with transcription, splicing, heterochromatin or nucleolar activity, respectively. Mitoxantrone was found to concentrate in MED1, FIB1 and NPM1 condensates, respectively, but not in BRD4, SRSF2 or HP1α condensates. JQ1 concentrated in MED1, BRD4 and NPM1 condensates, but not in SRSF2, HP1α or FIB1 condensates. The product of cisplatin activity, platinated DNA, was also observed in MED1 condensates in cells and DNA platination was dependent on MED1 condensates at some genomic loci. Tamoxifen was also observed in MED1 condensates in cells using an artificial system. Analysis of the types of molecules that concentrate in MED1 condensates, revealed enrichment of molecules with aromatic rings, suggesting that π-mediated interactions contribute to this phenomenon. Further, mutating aromatic residues in MED1 led to a decrease in concentration of some of these molecules. The activity of these molecules was enhanced by virtue of being in the condensate, as DNA platination was elevated in conditions conducive to MED1 condensation. These observations could be proven to be very useful in drug discovery. For example, one could envision designing drugs that will concentrate in a particular biomolecular condensate where the drug target lies to increase target engagement.

The age of condensate-targeted drug discovery is just at its inception, as is our understanding of how currently approved therapeutic agents interact with the structure and function of biomolecular condensates. It can be anticipated that the techniques and insights discussed in this manuscript will serve as a foundation to accelerate drug discovery and improve the efficacy of new therapeutics.

8 Conclusions and outlook into the future

Continuous developments in fluorescent labelling technologies and microscopy-based methods have enabled fast-paced progress in our collective understanding of the biophysics and biology of biomolecular condensates. Fluorescence probes have proved crucial in advancing the field, in particular the probes and methods that are compatible with live cell imaging and time-tracking applications. Major challenges are still experienced in the study of small, dynamic condensates without introducing external perturbations (i.e., overexpression, voluminous fluorescent tags, etc.), in order to facilitate their detection. In the future, focus is needed on advancements that allow visualization of small condensates, and methods to implement genetic tagging with the lowest impact on the condensate phenotype, such as sparce endogenous labelling, genetically encoded, un-natural amino acid incorporation, or other types of innocuous dyes and tags.

Acknowledgements

Raffi Manoukian is thanked for kindly sharing the fluorescence micrographs and segmentation images in Figs. 4 and 8; Dr. Jill Bouchard and Rebecca Zacks for help with the illustrations; Dr. Jill Bouchard and Raffi Manoukian for critical review and editing of the manuscript.

References

Adhikary, A., Buschmann, V., Muller, C., & Sauer, M. (2003). Ensemble and single-molecule fluorescence spectroscopic study of the binding modes of the bis-benzimidazole derivative Hoechst 33258 with DNA. *Nucleic Acids Research*, *31*, 2178–2186.

Alberti, S. (2017). The wisdom of crowds: Regulating cell function through condensed states of living matter. *Journal of Cell Science*, *130*, 2789–2796.

Alberti, S., & Dormann, D. (2019). Liquid-liquid phase separation in disease. *Annual Review of Genetics*, *53*, 171–194.

Alberti, S., Gladfelter, A., & Mittag, T. (2019). Considerations and challenges in studying liquid-liquid phase separation and biomolecular condensates. *Cell*, *176*, 419–434.

Alberti, S., Saha, S., Woodruff, J. B., Franzmann, T. M., Wang, J., & Hyman, A. A. (2018). A user's guide for phase separation assays with purified proteins. *Journal of Molecular Biology*, *430*, 4806–4820.

Andersen, J. S., Lam, Y. W., Leung, A. K., Ong, S. E., Lyon, C. E., Lamond, A. I., et al. (2005). Nucleolar proteome dynamics. *Nature*, *433*, 77–83.

Aulas, A., Fay, M. M., Lyons, S. M., Achorn, C. A., Kedersha, N., Anderson, P., et al. (2017). Stress-specific differences in assembly and composition of stress granules and related foci. *Journal of Cell Science*, *130*, 927–937.

Banani, S. F., Rice, A. M., Peeples, W. B., Lin, Y., Jain, S., Parker, R., et al. (2016). Compositional control of phase-separated cellular bodies. *Cell*, *166*, 651–663.

Bancaud, A., Huet, S., Daigle, N., Mozziconacci, J., Beaudouin, J., & Ellenberg, J. (2009). Molecular crowding affects diffusion and binding of nuclear proteins in heterochromatin and reveals the fractal organization of chromatin. *The EMBO Journal*, *28*, 3785–3798.

Batani, G., Bayer, K., Boge, J., Hentschel, U., & Thomas, T. (2019). Fluorescence in situ hybridization (FISH) and cell sorting of living bacteria. *Scientific Reports*, *9*, 18618.

Bausch, A. R., Ziemann, F., Boulbitch, A. A., Jacobson, K., & Sackmann, E. (1998). Local measurements of viscoelastic parameters of adherent cell surfaces by magnetic bead microrheometry. *Biophysical Journal*, *75*, 2038–2049.

Bertrand, E., Chartrand, P., Schaefer, M., Shenoy, S. M., Singer, R. H., & Long, R. M. (1998). Localization of ASH1 mRNA particles in living yeast. *Molecular Cell*, *2*, 437–445.

Bizzarri, R., Serresi, M., Cardarelli, F., Abbruzzetti, S., Campanini, B., Viappiani, C., et al. (2010). Single amino acid replacement makes Aequorea victoria fluorescent proteins reversibly photoswitchable. *Journal of the American Chemical Society*, *132*, 85–95.

Boeynaems, S., Holehouse, A. S., Weinhardt, V., Kovacs, D., Van Lindt, J., Larabell, C., et al. (2019). Spontaneous driving forces give rise to protein-RNA condensates with coexisting phases and complex material properties. *Proceedings of the National Academy of Sciences of the United States of America*, *116*, 7889–7898.

Boija, A., Klein, I. A., Sabari, B. R., Dall'Agnese, A., Coffey, E. L., Zamudio, A. V., et al. (2018). Transcription factors activate genes through the phase-separation capacity of their activation domains. *Cell*, *175*, 1842–1855, e1816.

Boisvert, F. M., van Koningsbruggen, S., Navascues, J., & Lamond, A. I. (2007). The multifunctional nucleolus. *Nature Reviews. Molecular Cell Biology*, *8*, 574–585.

Boothby, T. C., Tapia, H., Brozena, A. H., Piszkiewicz, S., Smith, A. E., Giovannini, I., et al. (2017). Tardigrades use intrinsically disordered proteins to survive desiccation. *Molecular Cell*, *65*, 975–984, e975.

Bouchard, J. J., Otero, J. H., Scott, D. C., Szulc, E., Martin, E. W., Sabri, N., et al. (2018). Cancer mutations of the tumor suppressor SPOP disrupt the formation of active, phase-separated compartments. *Molecular Cell*, *72*, 19–36, e18.

Bourgeois, D., & Adam, V. (2012). Reversible photoswitching in fluorescent proteins: A mechanistic view. *IUBMB Life*, *64*, 482–491.

Bracha, D., Walls, M. T., Wei, M. T., Zhu, L., Kurian, M., Avalos, J. L., et al. (2018). Mapping local and global liquid phase behavior in living cells using photo-oligomerizable seeds. *Cell*, *175*, 1467–1480, e1413.

Brangwynne, C. P., Eckmann, C. R., Courson, D. S., Rybarska, A., Hoege, C., Gharakhani, J., et al. (2009). Germline P granules are liquid droplets that localize by controlled dissolution/condensation. *Science*, *324*, 1729–1732.

Brangwynne, C. P., Mitchison, T. J., & Hyman, A. A. (2011). Active liquid-like behavior of nucleoli determines their size and shape in Xenopus laevis oocytes. *Proceedings of the National Academy of Sciences of the United States of America*, *108*, 4334–4339.

Bucevicius, J., Lukinavicius, G., & Gerasimaite, R. (2018). The use of Hoechst dyes for DNA staining and beyond. *Chemosensors*, *6*, 18.

Calloway, N. T., Choob, M., Sanz, A., Sheetz, M. P., Miller, L. W., & Cornish, V. W. (2007). Optimized fluorescent trimethoprim derivatives for in vivo protein labeling. *Chembiochem: A European Journal of Chemical Biology*, *8*, 767–774.

Cermakova, K., and Hodges, H.C. (2018). Next-generation drugs and probes for chromatin biology: From targeted protein degradation to phase separation. Molecules 23. 1958.

Cho, W. K., Spille, J. H., Hecht, M., Lee, C., Li, C., Grube, V., et al. (2018). Mediator and RNA polymerase II clusters associate in transcription-dependent condensates. *Science*, *361*, 412–415.

Chong, S., Dugast-Darzacq, C., Liu, Z., Dong, P., Dailey, G. M., Cattoglio, C., et al. (2018). Imaging dynamic and selective low-complexity domain interactions that control gene transcription. *Science, 361*.

Coons, A. H., Creech, H. J., Jones, R. N., & Berliner, E. (1942). Demonstration of pneumococcal antigen in tissues by the use of fluorescent antibody. *Journal of Immunology*, *45*, 159–170.

Costa, S. A., Simon, J. R., Amiram, M., Tang, L., Zauscher, S., Brustad, E. M., et al. (2018). Photo-crosslinkable unnatural amino acids enable facile synthesis of thermoresponsive nano- to microgels of intrinsically disordered polypeptides. *Advanced Materials, 30*. https://doi.org/10.1002/adma.201704878.

Cuevas-Velazquez, C. L., & Dinneny, J. R. (2018). Organization out of disorder: Liquid-liquid phase separation in plants. *Current Opinion in Plant Biology*, *45*, 68–74.

Delarue, M., Brittingham, G. P., Pfeffer, S., Surovtsev, I. V., Pinglay, S., Kennedy, K. J., et al. (2018). mTORC1 controls phase separation and the biophysical properties of the cytoplasm by tuning crowding. *Cell*, *174*, 338–349, e320.

Duim, W. C., Chen, B., Frydman, J., & Moerner, W. E. (2011). Sub-diffraction imaging of huntingtin protein aggregates by fluorescence blink-microscopy and atomic force microscopy. *ChemPhysChem*, *12*, 2387–2390.

Eissing, N., Heger, L., Baranska, A., Cesnjevar, R., Buttner-Herold, M., Soder, S., et al. (2014). Easy performance of 6-color confocal immunofluorescence with 4-laser line microscopes. *Immunology Letters*, *161*, 1–5.

Elbaum-Garfinkle, S., Kim, Y., Szczepaniak, K., Chen, C. C., Eckmann, C. R., Myong, S., et al. (2015). The disordered P granule protein LAF-1 drives phase separation into droplets with tunable viscosity and dynamics. *Proceedings of the National Academy of Sciences of the United States of America*, *112*, 7189–7194.

Fei, J., Jadaliha, M., Harmon, T. S., Li, I. T. S., Hua, B., Hao, Q., et al. (2017). Quantitative analysis of multilayer organization of proteins and RNA in nuclear speckles at super resolution. *Journal of Cell Science*, *130*, 4180–4192.

Femino, A. M., Fay, F. S., Fogarty, K., & Singer, R. H. (1998). Visualization of single RNA transcripts in situ. *Science*, *280*, 585–590.

Feric, M., Vaidya, N., Harmon, T. S., Mitrea, D. M., Zhu, L., Richardson, T. M., et al. (2016). Coexisting liquid phases underlie nucleolar subcompartments. *Cell*, *165*, 1686–1697.

Fernandez-Suarez, M., Baruah, H., Martinez-Hernandez, L., Xie, K. T., Baskin, J. M., Bertozzi, C. R., et al. (2007). Redirecting lipoic acid ligase for cell surface protein labeling with small-molecule probes. *Nature Biotechnology*, *25*, 1483–1487.

Ferrolino, M. C., Mitrea, D. M., Michael, J. R., & Kriwacki, R. W. (2018). Compositional adaptability in NPM1-SURF6 scaffolding networks enabled by dynamic switching of phase separation mechanisms. *Nature Communications*, *9*, 5064.

Fusco, D., Accornero, N., Lavoie, B., Shenoy, S. M., Blanchard, J. M., Singer, R. H., et al. (2003). Single mRNA molecules demonstrate probabilistic movement in living mammalian cells. *Current Biology*, *13*, 161–167.

Gallagher, S. S., Sable, J. E., Sheetz, M. P., & Cornish, V. W. (2009). An in vivo covalent TMP-tag based on proximity-induced reactivity. *ACS Chemical Biology*, *4*, 547–556.

Gautier, A., Juillerat, A., Heinis, C., Correa, I. R., Jr., Kindermann, M., Beaufils, F., et al. (2008). An engineered protein tag for multiprotein labeling in living cells. *Chemistry & Biology*, *15*, 128–136.

Gurskaya, N. G., Verkhusha, V. V., Shcheglov, A. S., Staroverov, D. B., Chepurnykh, T. V., Fradkov, A. F., et al. (2006). Engineering of a monomeric green-to-red photoactivatable fluorescent protein induced by blue light. *Nature Biotechnology*, *24*, 461–465.

Gut, G., Herrmann, M. D., & Pelkmans, L. (2018). Multiplexed protein maps link subcellular organization to cellular states. *Science*, *361*, eaar7042.

Han, F., Taulier, N., & Chalikian, T. V. (2005). Association of the minor groove binding drug Hoechst 33258 with d(CGCGAATTCGCG)2: Volumetric, calorimetric, and spectroscopic characterizations. *Biochemistry*, *44*, 9785–9794.

Heinis, C., Schmitt, S., Kindermann, M., Godin, G., & Johnsson, K. (2006). Evolving the substrate specificity of O6-alkylguanine-DNA alkyltransferase through loop insertion for applications in molecular imaging. *ACS Chemical Biology*, *1*, 575–584.

Hobson, C. M., O'Brien, E. T., 3rd, Falvo, M. R., & Superfine, R. (2020). Combined selective plane illumination microscopy and FRAP maps intranuclear diffusion of NLS-GFP. *Biophysical Journal*, *119*, 514–524.https://www.nobelprize.org/prizes/chemistry/2008/summary.

Hubstenberger, A., Courel, M., Benard, M., Souquere, S., Ernoult-Lange, M., Chouaib, R., et al. (2017). P-body purification reveals the condensation of repressed mRNA regulons. *Molecular Cell*, *68*, 144–157, e145.

Hyman, A. A., Weber, C. A., & Julicher, F. (2014). Liquid-liquid phase separation in biology. *Annual Review of Cell and Developmental Biology*, *30*, 39–58.

Jain, A., & Vale, R. D. (2017). RNA phase transitions in repeat expansion disorders. *Nature*, *546*, 243–247.

Jain, S., Wheeler, J. R., Walters, R. W., Agrawal, A., Barsic, A., & Parker, R. (2016). ATPase-modulated stress granules contain a diverse proteome and substructure. *Cell*, *164*, 487–498.

Janicki, S. M., Tsukamoto, T., Salghetti, S. E., Tansey, W. P., Sachidanandam, R., Prasanth, K. V., et al. (2004). From silencing to gene expression: Real-time analysis in single cells. *Cell*, *116*, 683–698.

Jawerth, L. M., Ijavi, M., Ruer, M., Saha, S., Jahnel, M., Hyman, A. A., et al. (2018). Salt-dependent rheology and surface tension of protein condensates using optical traps. *Physical Review Letters*, *121*, 258101.

Khong, A., Matheny, T., Jain, S., Mitchell, S. F., Wheeler, J. R., & Parker, R. (2017). The stress granule transcriptome reveals principles of mRNA accumulation in stress granules. *Molecular Cell*, *68*, 808–820, e805.

Kishi, J. Y., Lapan, S. W., Beliveau, B. J., West, E. R., Zhu, A., Sasaki, H. M., et al. (2019). SABER amplifies FISH: Enhanced multiplexed imaging of RNA and DNA in cells and tissues. *Nature Methods*, *16*, 533–544.

Klein, I. A., Boija, A., Afeyan, L. K., Hawken, S. W., Fan, M., Dall'Agnese, A., et al. (2020). Partitioning of cancer therapeutics in nuclear condensates. *Science*, *368*, 1386–1392.

Kroschwald, S., Maharana, S., & Alberti, S. (2017). Hexanediol: A chemical probe to investigate the material properties of membrane-less compartments. *Matters*, 1–7.

Ladouceur, A. M., Parmar, B. S., Biedzinski, S., Wall, J., Tope, S. G., Cohn, D., et al. (2020). Clusters of bacterial RNA polymerase are biomolecular condensates that assemble through liquid-liquid phase separation. *Proceedings of the National Academy of Sciences of the United States of America*, *117*, 18540–18549.

Laine, R. F., Sinnige, T., Ma, K. Y., Haack, A. J., Poudel, C., Gaida, P., et al. (2019). Fast fluorescence lifetime imaging reveals the aggregation processes of alpha-Synuclein and Polyglutamine in aging Caenorhabditis elegans. *ACS Chemical Biology*, *14*, 1628–1636.

Lambert, T. J. (2019). FPbase: A community-editable fluorescent protein database. *Nature Methods*, *16*, 277–278.

Langdon, E. M., Qiu, Y., Ghanbari Niaki, A., McLaughlin, G. A., Weidmann, C. A., Gerbich, T. M., et al. (2018). mRNA structure determines specificity of a polyQ-driven phase separation. *Science*, *360*, 922–927.

Lee, C., Occhipinti, P., & Gladfelter, A. S. (2015). PolyQ-dependent RNA-protein assemblies control symmetry breaking. *The Journal of Cell Biology*, *208*, 533–544.

Lee, C. S., Putnam, A., Lu, T., He, S., Ouyang, J. P. T., & Seydoux, G. (2020). Recruitment of mRNAs to P granules by condensation with intrinsically-disordered proteins. *Elife*, *9*, e52896.

Lemos, C., Schulze, L., Weiske, J., Meyer, H., Braeuer, N., Barak, N., et al. (2020). Identification of small molecules that modulate mutant p53 condensation. *iScience, 23*, 101517.

Li, P., Banjade, S., Cheng, H. C., Kim, S., Chen, B., Guo, L., et al. (2012). Phase transitions in the assembly of multivalent signalling proteins. *Nature*, *483*, 336–340.

Li, C. H., Coffey, E. L., Dall'Agnese, A., Hannett, N. M., Tang, X., Henninger, J. E., et al. (2020). MeCP2 links heterochromatin condensates and neurodevelopmental disease. *Nature*, *586*, 440–444.

Linsenmeier, M., Kopp, M. R. G., Stavrakis, S., de Mello, A., & Arosio, P. (2020). Analysis of biomolecular condensates and protein phase separation with microfluidic technology. *Biochimica et Biophysica Acta (BBA)—Molecular Cell Research*, *1868*, 118823.

Liu, H., Dong, P., Ioannou, M. S., Li, L., Shea, J., Pasolli, H. A., et al. (2018). Visualizing long-term single-molecule dynamics in vivo by stochastic protein labeling. *Proceedings of the National Academy of Sciences of the United States of America*, *115*, 343–348.

Los, G. V., & Wood, K. (2007). The HaloTag: A novel technology for cell imaging and protein analysis. *Methods in Molecular Biology*, *356*, 195–208.

Louvet, E., Yoshida, A., Kumeta, M., & Takeyasu, K. (2014). Probing the stiffness of isolated nucleoli by atomic force microscopy. *Histochemistry and Cell Biology*, *141*, 365–381.

Mahboubi, H., & Stochaj, U. (2017). Cytoplasmic stress granules: Dynamic modulators of cell signaling and disease. *Biochimica et Biophysica Acta—Molecular Basis of Disease*, *1863*, 884–895.

Markmiller, S., Soltanieh, S., Server, K. L., Mak, R., Jin, W., Fang, M. Y., et al. (2018). Context-dependent and disease-specific diversity in protein interactions within stress granules. *Cell*, *172*, 590–604, e513.

Martin, E. W., Holehouse, A. S., Peran, I., Farag, M., Incicco, J. J., Bremer, A., et al. (2020). Valence and patterning of aromatic residues determine the phase behavior of prion-like domains. *Science*, *367*, 694–699.

Martin, R. M., Ter-Avetisyan, G., Herce, H. D., Ludwig, A. K., Lattig-Tunnemann, G., & Cardoso, M. C. (2015). Principles of protein targeting to the nucleolus. *Nucleus*, *6*, 314–325.

Miao, K., & Wei, L. (2020). Live-cell imaging and quantification of PolyQ aggregates by stimulated Raman scattering of selective deuterium labeling. *ACS Central Science*, *6*, 478–486.

Miller, L. W., Cai, Y., Sheetz, M. P., & Cornish, V. W. (2005). In vivo protein labeling with trimethoprim conjugates: A flexible chemical tag. *Nature Methods*, *2*, 255–257.

Mitrea, D. M., Chandra, B., Ferrolino, M. C., Gibbs, E. B., Tolbert, M., White, M. R., et al. (2018). Methods for physical characterization of phase-separated bodies and membraneless organelles. *Journal of Molecular Biology*, *430*, 4773–4805.

Mitrea, D. M., Cika, J. A., Guy, C. S., Ban, D., Banerjee, P. R., Stanley, C. B., et al. (2016). Nucleophosmin integrates within the nucleolus via multi-modal interactions with proteins displaying R-rich linear motifs and rRNA. *eLife*, *5*, e13571.

Mitrea, D. M., Cika, J. A., Stanley, C. B., Nourse, A., Onuchic, P. L., Banerjee, P. R., et al. (2018). Self-interaction of NPM1 modulates multiple mechanisms of liquid-liquid phase separation. *Nature Communications*, *9*, 842.

Mitrea, D. M., & Kriwacki, R. W. (2016). Phase separation in biology; functional organization of a higher order. *Cell Communication and Signaling: CCS*, *14*, 1.

Mittasch, M., Gross, P., Nestler, M., Fritsch, A. W., Iserman, C., Kar, M., et al. (2018). Non-invasive perturbations of intracellular flow reveal physical principles of cell organization. *Nature Cell Biology*, *20*, 344–351.

Mittasch, M., Tran, V. M., Rios, M. U., Fritsch, A. W., Enos, S. J., Ferreira Gomes, B., et al. (2020). Regulated changes in material properties underlie centrosome disassembly during mitotic exit. *The Journal of Cell Biology*, *219*, e201912036.

Molliex, A., Temirov, J., Lee, J., Coughlin, M., Kanagaraj, A. P., Kim, H. J., et al. (2015). Phase separation by low complexity domains promotes stress granule assembly and drives pathological fibrillization. *Cell*, *163*, 123–133.

Morikawa, T. J., Fujita, H., Kitamura, A., Horio, T., Yamamoto, J., Kinjo, M., et al. (2016). Dependence of fluorescent protein brightness on protein concentration in solution and enhancement of it. *Scientific Reports*, *6*, 22342.

Munder, M. C., Midtvedt, D., Franzmann, T., Nuske, E., Otto, O., Herbig, M., et al. (2016). A pH-driven transition of the cytoplasm from a fluid- to a solid-like state promotes entry into dormancy. *eLife*, *5*, e09347.

Muramatsu, M., & Onishi, T. (1978). Isolation and purification of nucleoli and nucleolar chromatin from mammalian cells. *Methods in Cell Biology*, *17*, 141–161.

Newman, J., Peat, T. S., Richard, R., Kan, L., Swanson, P. E., Affholter, J. A., et al. (1999). Haloalkane dehalogenases: Structure of a Rhodococcus enzyme. *Biochemistry*, *38*, 16105–16114.

Nodling, A. R., Spear, L. A., Williams, T. L., Luk, L. Y. P., & Tsai, Y. H. (2019). Using genetically incorporated unnatural amino acids to control protein functions in mammalian cells. *Essays in Biochemistry*, *63*, 237–266.

Nott, T. J., Petsalaki, E., Farber, P., Jervis, D., Fussner, E., Plochowietz, A., et al. (2015). Phase transition of a disordered nuage protein generates environmentally responsive membraneless organelles. *Molecular Cell*, *57*, 936–947.

Padron, A., Iwasaki, S., & Ingolia, N. T. (2019). Proximity RNA labeling by APEX-Seq reveals the organization of translation initiation complexes and repressive RNA granules. *Molecular Cell*, *75*, 875–887, e875.

Pak, C. W., Kosno, M., Holehouse, A. S., Padrick, S. B., Mittal, A., Ali, R., et al. (2016). Sequence determinants of intracellular phase separation by complex coacervation of a disordered protein. *Molecular Cell*, *63*, 72–85.

Pardue, M. L., & Gall, J. G. (1969). Molecular hybridization of radioactive DNA to the DNA of cytological preparations. *Proceedings of the National Academy of Sciences of the United States of America*, *64*, 600–604.

Patel, A., Lee, H. O., Jawerth, L., Maharana, S., Jahnel, M., Hein, M. Y., et al. (2015). A liquid-to-solid phase transition of the ALS protein FUS accelerated by disease mutation. *Cell*, *162*, 1066–1077.

Patterson, G. H., & Lippincott-Schwartz, J. (2002). A photoactivatable GFP for selective photolabeling of proteins and cells. *Science*, *297*, 1873–1877.

Picardi, G., Spalloni, A., Generosi, A., Paci, B., Mercuri, N. B., Luce, M., et al. (2018). Tissue degeneration in ALS affected spinal cord evaluated by Raman spectroscopy. *Scientific Reports*, *8*, 13110.

Poser, I., Sarov, M., Hutchins, J. R., Heriche, J. K., Toyoda, Y., Pozniakovsky, A., et al. (2008). BAC TransgeneOmics: A high-throughput method for exploration of protein function in mammals. *Nature Methods*, *5*, 409–415.

Putnam, A., Cassani, M., Smith, J., & Seydoux, G. (2019). A gel phase promotes condensation of liquid P granules in Caenorhabditis elegans embryos. *Nature Structural & Molecular Biology*, *26*, 220–226.

Reed, E. H., Schuster, B. S., Good, M. C., & Hammer, D. A. (2020). SPLIT: Stable protein coacervation using a light induced transition. *ACS Synthetic Biology*, *9*, 500–507.

Riback, J. A., Katanski, C. D., Kear-Scott, J. L., Pilipenko, E. V., Rojek, A. E., Sosnick, T. R., et al. (2017). Stress-triggered phase separation is an adaptive, evolutionarily tuned response. *Cell*, *168*, 1028–1040, e1019.

Riback, J. A., Zhu, L., Ferrolino, M. C., Tolbert, M., Mitrea, D. M., Sanders, D. W., et al. (2020). Composition-dependent thermodynamics of intracellular phase separation. *Nature*, *581*, 209–214.

Robinett, C. C., Straight, A., Li, G., Willhelm, C., Sudlow, G., Murray, A., et al. (1996). In vivo localization of DNA sequences and visualization of large-scale chromatin organization using lac operator/repressor recognition. *The Journal of Cell Biology*, *135*, 1685–1700.

Rodriguez-Rodriguez, D. R., Ramirez-Solis, R., Garza-Elizondo, M. A., Garza-Rodriguez, M. L., & Barrera-Saldana, H. A. (2019). Genome editing: A perspective on the application of CRISPR/Cas9 to study human diseases (review). *International Journal of Molecular Medicine*, *43*, 1559–1574.

Sabari, B. R., Dall'Agnese, A., & Young, R. A. (2020). Biomolecular condensates in the nucleus. *Trends in Biochemical Sciences*, *45*(11), 961–977.

Shen, Y., Ruggeri, F. S., Vigolo, D., Kamada, A., Qamar, S., Levin, A., et al. (2020). Biomolecular condensates undergo a generic shear-mediated liquid-to-solid transition. *Nature Nanotechnology*, *15*, 841–847.

Shimomura, O., Johnson, F. H., & Saiga, Y. (1962). Extraction, purification and properties of aequorin, a bioluminescent protein from the luminous hydromedusan, Aequorea. *Journal of Cellular and Comparative Physiology*, *59*, 223–239.

Shin, Y., Berry, J., Pannucci, N., Haataja, M. P., Toettcher, J. E., & Brangwynne, C. P. (2017). Spatiotemporal control of intracellular phase transitions using light-activated optoDroplets. *Cell*, *168*, 159–171, e114.

Shin, Y., & Brangwynne, C. P. (2017). Liquid phase condensation in cell physiology and disease. *Science*, *357*, eaaf4382.

Shin, Y., Chang, Y. C., Lee, D. S. W., Berry, J., Sanders, D. W., Ronceray, P., et al. (2018). Liquid nuclear condensates mechanically sense and restructure the genome. *Cell*, *175*, 1481–1491, e1413.

Sinnamon, J. R., & Czaplinski, K. (2014). RNA detection in situ with FISH-STICs. *RNA*, *20*, 260–266.

Slavoff, S. A., Chen, I., Choi, Y. A., & Ting, A. Y. (2008). Expanding the substrate tolerance of biotin ligase through exploration of enzymes from diverse species. *Journal of the American Chemical Society*, *130*, 1160–1162.

Stiel, A. C., Andresen, M., Bock, H., Hilbert, M., Schilde, J., Schonle, A., et al. (2008). Generation of monomeric reversibly switchable red fluorescent proteins for far-field fluorescence nanoscopy. *Biophysical Journal*, *95*, 2989–2997.

Stracy, M., Lesterlin, C., Garza de Leon, F., Uphoff, S., Zawadzki, P., & Kapanidis, A. N. (2015). Live-cell superresolution microscopy reveals the organization of RNA polymerase in the bacterial nucleoid. *Proceedings of the National Academy of Sciences of the United States of America*, *112*, E4390–E4399.

Strom, A. R., Emelyanov, A. V., Mir, M., Fyodorov, D. V., Darzacq, X., & Karpen, G. H. (2017). Phase separation drives heterochromatin domain formation. *Nature*, *547*, 241–245.

Sydor, A. M., Czymmek, K. J., Puchner, E. M., & Mennella, V. (2015). Super-resolution microscopy: From single molecules to supramolecular assemblies. *Trends in Cell Biology*, *25*, 730–748.

Taylor, N. O., Wei, M. T., Stone, H. A., & Brangwynne, C. P. (2019). Quantifying dynamics in phase-separated condensates using fluorescence recovery after Photobleaching. *Biophysical Journal*, *117*, 1285–1300.

Trotta, E. (2016). Selective forces and mutational biases drive stop codon usage in the human genome: A comparison with sense codon usage. *BMC Genomics*, *17*, 366.

Uhlen, M., Bandrowski, A., Carr, S., Edwards, A., Ellenberg, J., Lundberg, E., et al. (2016). A proposal for validation of antibodies. *Nature Methods*, *13*, 823–827.

Wang, J., Choi, J. M., Holehouse, A. S., Lee, H. O., Zhang, X., Jahnel, M., et al. (2018). A molecular grammar governing the driving forces for phase separation of prion-like RNA binding proteins. *Cell*, *174*, 688–699, e616.

Wang, J. T., Smith, J., Chen, B. C., Schmidt, H., Rasoloson, D., Paix, A., et al. (2014). Regulation of RNA granule dynamics by phosphorylation of serine-rich, intrinsically disordered proteins in *C. elegans*. *Elife*, *3*, e04591.

Weber, S. C., & Brangwynne, C. P. (2015). Inverse size scaling of the nucleolus by a concentration-dependent phase transition. *Current Biology*, *25*, 641–646.

Wei, M. T., Chang, Y. C., Shimobayashi, S. F., Shin, Y., Strom, A. R., & Brangwynne, C. P. (2020). Nucleated transcriptional condensates amplify gene expression. *Nature Cell Biology*, *22*, 1187–1196.

Wei, M. T., Elbaum-Garfinkle, S., Holehouse, A. S., Chen, C. C., Feric, M., Arnold, C. B., et al. (2017). Phase behaviour of disordered proteins underlying low density and high permeability of liquid organelles. *Nature Chemistry*, *9*, 1118–1125.

Wheeler, J. R., Jain, S., Khong, A., & Parker, R. (2017). Isolation of yeast and mammalian stress granule cores. *Methods*, *126*, 12–17.

Wheeler, J. R., Lee, H. O., Poser, I., Pal, A., Doeleman, T., Kishigami, S., et al. (2019). Small molecules for modulating protein driven liquid-liquid phase separation in treating neurodegenerative disease. *bioRxiv*.

Woodruff, J. B., Ferreira Gomes, B., Widlund, P. O., Mahamid, J., Honigmann, A., & Hyman, A. A. (2017). The centrosome is a selective condensate that nucleates microtubules by concentrating tubulin. *Cell*, *169*, 1066–1077, e1010.

Wu, B., Chen, J., & Singer, R. H. (2014). Background free imaging of single mRNAs in live cells using split fluorescent proteins. *Scientific Reports*, *4*, 3615.

Xia, C., Babcock, H. P., Moffitt, J. R., & Zhuang, X. (2019). Multiplexed detection of RNA using MERFISH and branched DNA amplification. *Scientific Reports*, *9*, 7721.

Xia, C., Fan, J., Emanuel, G., Hao, J., & Zhuang, X. (2019). Spatial transcriptome profiling by MERFISH reveals subcellular RNA compartmentalization and cell cycle-dependent gene expression. *Proceedings of the National Academy of Sciences of the United States of America*, *116*, 19490–19499.

Xing, W., Muhlrad, D., Parker, R., & Rosen, M. K. (2020). A quantitative inventory of yeast P body proteins reveals principles of composition and specificity. *eLife*, *9*, e56525.

Yasuda, S., Tsuchiya, H., Kaiho, A., Guo, Q., Ikeuchi, K., Endo, A., et al. (2020). Stress- and ubiquitylation-dependent phase separation of the proteasome. *Nature*, *578*, 296–300.

Zamudio, A. V., Dall'Agnese, A., Henninger, J. E., Manteiga, J. C., Afeyan, L. K., Hannett, N. M., et al. (2019). Mediator condensates localize signaling factors to key cell identity genes. *Molecular Cell*, *76*, 753–766, e756.

Zhang, H., Zhao, R., Tones, J., Liu, M., Dilley, R. L., Chenoweth, D. M., et al. (2020). Nuclear body phase separation drives telomere clustering in ALT cancer cells. *Molecular Biology of the Cell*, *31*, 2048–2056.

Zhao, Y. G., & Zhang, H. (2020). Phase separation in membrane biology: The interplay between membrane-bound organelles and Membraneless condensates. *Developmental Cell*, *55*, 30–44.

Zhu, L., Richardson, T. M., Wacheul, L., Wei, M. T., Feric, M., Whitney, G., et al. (2019). Controlling the material properties and rRNA processing function of the nucleolus using light. *Proceedings of the National Academy of Sciences of the United States of America*, *116*, 17330–17335.

Zia, R. N. (2018). Active and passive microrheology: Theory and simulation. *Annual Review of Fluid Mechanics*, *50*, 371–405.